View metadata, citation and similar papers at core.ac.uk

brought to you by CORE

provided by NASA Technical Reports Server

NASA TECHNICAL NOTE

NASA TN D-7500

NASA TN D-7500

(NASA-TN-D-7500) A FINE POINTING SYSTEM FOR THE LARGE SPACE TELESCOPE (NASA) 75 p HC $3 50 CSCL 03A

N74-14507

Unclas

H1/30 25275

A FINE POINTING SYSTEM FOR THE LARGE SPACE TELESCOPE

by Werner O. Schiehlen

George C. Marshall Space Flight Center

Marshall Space Flight Center, Ala. 35812

NATIONAL AERONAUTICS AND SPACE ADMINISTRATION • WASHINGTON, D. C. • DECEMBER 1973

1. REPORT NO.	2. GOVERNMENT ACCESSION NO.	3. RECIPIENT'S CATALOG NO.
NASA TN D-7500		

4. TITLE AND SUBTITLE	5. REPORT DATE
A Fine Pointing System for the Large Space Telescope	December 1973
	6. PERFORMING ORGANIZATION CODE
7. AUTHOR(S)	8. PERFORMING ORGANIZATION REPORT #
Werner O. Schiehlen*	M217
9. PERFORMING ORGANIZATION NAME AND ADDRESS	10. WORK UNIT NO.
George C. Marshall Space Flight Center Marshall Space Flight Center, Alabama 35812	11. CONTRACT OR GRANT NO.
	13. TYPE OF REPORT & PERIOD COVERED
12. SPONSORING AGENCY NAME AND ADDRESS	Technical Note
National Aeronautics and Space Administration Washington, D.C. 20546	14. SPONSORING AGENCY CODE

15. SUPPLEMENTARY NOTES

Prepared by Astrionics Laboratory, Science and Engineering

*National Research Council, National Academy of Sciences, Washington, D.C.

16. ABSTRACT

The Large Space Telescope (LST) developed by NASA requires ultra-high pointing stability within 0.005 arc sec rms. A fine guidance system is proposed to body-point the entire spacecraft within this limit. The spacecraft is modeled as a rigid body having reaction wheel actuators and subject to gravitational and magnetic disturbance torques. The fine guidance sensor is cluttered with electronic noise. The Disturbance Accommodation Standard deviation Optimal Controller (DASOC) is designed to be optimal with respect to the transient and the steady-state response to noise, whereas the steady-state response to deterministic external torques is exactly zero. Compared with conventional controllers, the fine guidance system with the DASOC offers as much as a factor of 30 improvement in pointing stability, resulting in an optimal performance of nearly 0.0001 arc sec rms. Thus, the required pointing stability can easily be obtained, and a large margin remains for the compensation of possible deteriorations.

17. KEY WORDS	18. DISTRIBUTION STATEMENT

19. SECURITY CLASSIF. (of this report)	20. SECURITY CLASSIF. (of this page)	21. NO. OF PAGES	22. PRICE
Unclassified	Unclassified	74	Domestic, $3.50 Foreign, $6.00

MSFC - Form 3292 (Rev December 1972) For sale by National Technical Information Service, Springfield, Virginia 22151

ACKNOWLEDGMENT

The author gratefully acknowledges the advice of Dr. Gerald S. Nurre of the Astrionics Laboratory at the George C. Marshall Space Flight Center and the support of the National Research Council, National Academy of Sciences, Washington, D.C., as well as the supplementary support of the Deutsche Forschungsgemeinschaft, Bonn-Bad Godesberg, Germany.

TABLE OF CONTENTS

PRECEDING PAGE BLANK NOT FILMED

LIST OF ILLUSTRATIONS

LIST OF TABLES

DEFINITION OF SYMBOLS

Symbol	Definition
A	2 × 2-open-loop system matrix (LST)
$\bar{A}$	7 × 7-closed-loop system matrix (LST and DASOC)
A_m	7 × 7-auxiliary matrix, m = 0(1)6
${}^{OI}A,\ {}^{IS}A$	3 × 3-transformation matrix between frames O,I and I,S
a_i	Coefficient of characteristic equation, i = 1(1)7
a_{ij}	Element of the transformation matrix ${}^{OI}A$, i = 1(1)3, j = 1(1)3
B	2 × 1-control matrix (LST)
B_o	Earth's magnetic field intensity
${}_o\underline{B},\ \underline{B}$	Earth's magnetic field intensity vector in frames O and S
b	Control constant
C	1 × 2-sensor matrix (LST)
c	Regulator gain
D	3 × 3-disturbance model matrix
d	Regulator gain
d_o	Delay constant
E	7 × 7-unit matrix
$E\{x\}$	Expectation of x
$\underline{e}_m$	Unit vector of the LST dipole moment in frame S
${}_o\underline{e}_V,\ \underline{e}_V$	Unit vector of orbit radius in frames O and S
F	2 × 1-deterministic disturbance matrix (LST)

DEFINITION OF SYMBOLS (Continued)

Symbol	Definition
$\bar{F}$	7 × 1-deterministic disturbance matrix (LST and DASOC)
f	Complex amplitude of sinusoidal disturbance
G	2 × 1-stochastic disturbance matrix (LST)
$\bar{G}$	7 × 2-stochastic disturbance matrix (LST and DASOC)
g	7 × 1-stochastic vector of sinusoidal response
g_{xi}, g_{yi}, g_{zi}	Gravity-gradient torque coefficients, i = 1, 2
H	1 × 3-disturbance matrix in section, Disturbance Accomodation Control System Design
H	7 × 7-Hurwitz matrix in sections, Stability and Transient Response, and Optimization of the Noise Response
H_i	Principal minor of Hurwitz matrix H, i = 1(1)7
$H_{k+1,1}$	Cofactor of the element $h_{k+1,1}$ of Hurwitz matrix, k = 0(1)6
h_{xi}, h_{yi}, h_{zi}	Magnetic torque coefficients, i = 1, 2
I_x, I_y, I_z	LST principal moments of inertia
I_{ix}, I_{iy}, I_{iz}	Reaction wheel principal moments of inertia, i = 1(1)3
$\underline{I}$	LST inertia tensor in frame S
$\underline{I}_i$	Reaction wheel inertia tensor in frame S, i = 1(1)3
i	Orbital inclination in section, Description of the LST Model
i	$\sqrt{-1}$ in section, Sensitivity Analysis of the DASOC System
K_1	1 × 2-observer parameter matrix
K_2	1 × 3-accommodator parameter matrix

DEFINITION OF SYMBOLS (Continued)

Symbol	Definition
k	Drive motor constant
k_i	Observer and accommodator gains, i = 1(1)5
L	1 × 2-regulator parameter matrix
M_x, M_y, M_z	External torques
M_{1x}, M_{2y}, M_{3z}	Internal torques
$\underline{M}$	External torque vector in frame S
$\underline{M}_{as}$	Aerodynamic and solar pressure torque
$\underline{M}_i$	Internal torque vector in frame S
$\underline{M}_g$	Gravity-gradient torque vector in frame S
$\underline{M}_m$	Magnetic torque vector in frame S
m_o	Dipole moment magnitude
m_v	Guide star magnitude
$\underline{m}$	Dipole moment vector in frame S
P, P_0	7 × 7-covariance matrix
Q	7 × 7-generalized spectral density matrix
q	Spectral density of stochastic disturbance
R	7 × 1-complex frequency response matrix
rms_θ	Root mean square error of pitch motion, pointing stability
r	Spectral density of sensor noise
S	2 × 2-spectral density matrix

DEFINITION OF SYMBOLS (Continued)

Symbol	Definition
s	1×1-stochastic disturbance vector
t	Time
u, u_c, u_r	1×1-control vector
u_o	Real part of complex denominator
V	2×1-generalized noise excitation vector (LST and DASOC)
v	1×1-sensor noise vector (LST)
v_o	Imaginary part of complex denominator
W, W_β, W_γ	1×1-generalized deterministic disturbance vector (LST and DASOC)
$w, \hat{w}$	1×1-deterministic disturbance vector (LST)
X, X_o	7×1-generalized state vector (LST and DASOC)
$\overline{X}, \overline{X}_o$	7×1-generalized mean vector
X_β, X_γ	7×1-generalized steady-state vector
$x, \hat{x}$	2×1-state vector (LST)
x_i	Real part of complex numerator
y	1×1-sensor vector (LST)
y_i	Imaginary part of complex numerator
$z, \hat{z}$	3×1-disturbance state vector
α	Characteristic frequency
β	Magnitude of constant disturbance
Γ	1×1-cancellation matrix

DEFINITION OF SYMBOLS (Continued)

Symbol	Definition
γ, γ_c, γ_s	Amplitude of sinusoidal disturbance
ϵ	Orbital rate error
θ	Pitch angle
κ_i	Coefficients i = 1(1)4
λ_i	Eigenvalues i = 1(1)7
ν_1, ν_2, ν_3	Relative angular velocity of reaction wheels
ξ_i, ξ_{ci}, ξ_{si}	Amplitude of frequency response, i = 1(1)7
ξ_θ	Amplitude of pitch motion
ρ	Guide star offset
σ_{xi}	Standard deviation i = 1(1)7
σ_θ	Standard deviation of pitch motion, pointing stability
τ	Angle locating LST in orbit
ϕ	Roll angle
χ, χ_i	Phase angle
ψ	Yaw angle
ω	Twice orbital rate
$\underline{\omega}$	Angular velocity of LST in frame S
$\underline{\omega}_i$	Relative angular velocity of reaction wheels in frame S, i = 1(1)3
Ω	Arbitrary frequency

DEFINITION OF SYMBOLS (Continued)

Appendix

Symbol	Definition
A	$n \times n$-system matrix
A_m	$n \times n$-auxiliary matrix, $m = 0(1)n-1$
a_i	Coefficient of characteristic equation, $i = 0(1)n$
B	$n \times$ r-excitation matrix
b_i	Coefficient of polynomial, $i = 0(1)n-1$
C	$n(n-1)/2 \times n(n-1)/2$ – Chen and Shieh matrix
$E\{x\}$	Expectation of x
E	$n \times n$-unit matrix
F	$n \times$ r-frequency response matrix
g_n	Polynomial
H	$n \times n$-Hurwitz matrix
$H_{k+1,1}$	Cofactor of the element $h_{k+1,1}$ of Hurwitz matrix, $k = 0(1)\ n-1$.
h_n	Characteristic equation
i	$\sqrt{-1}$
m, m_0, m_∞	$n \times 1$-mean vector
P, P_0, P_∞	$n \times n$-covariance matrix
p	$n(n-1)/2 \times 1$-vector of elements of P
Q	$r \times$ r-spectral density matrix
q	$n(n-1)/2 \times 1$-vector of elements of BQB^T

DEFINITION OF SYMBOLS (Concluded)

Symbol	Definition
S_w	r X r-spectral density matrix
S_x	n X n-spectral density matrix
s	Operator
t	Time
w	r X 1-disturbance vector
x, x_0	n X 1-state vector
$\delta(t)$	Delta function
λ_i, λ_j	Eigenvalues, i = 1(1)n , j = 1(1)n
τ	Time
Φ	n X n-fundamental matrix
ω	Frequency

NONSTANDARD ABBREVIATIONS

DASOC	Disturbance Accommodation Standard deviation Optimal Controller
PC	Proportional Controller
PIC	Proportional Integral Controller
PI^2C	Proportional Integral Squared Controller

A FINE POINTING SYSTEM FOR THE LARGE SPACE TELESCOPE

INTRODUCTION

The Large Space Telescope (LST) is to be an astronomical facility developed by the National Aeronautics and Space Administration (NASA) under the direction of the George C. Marshall Space Flight Center (MSFC), Huntsville, Alabama. The LST is the next step for optical stellar space astronomy after the Orbital Astronomical Observatories (OAO) and the Apollo Telescope Mount (ATM). It will be designed as a general-purpose facility, capable of utilizing a wide range of scientific instruments. The LST is expected to contribute significantly to studies relevant to the origin and structure of the universe, the study of energy processes that occur in galactic nuclei, the study of early stages of stellar and solar systems, and observation of such highly evolved objects as supernova remnants and white dwarfs. The LST will be capable of viewing galaxies 100 times fainter than those seen by the most powerful ground-based optical telescopes. It will weigh between 9000 and 11 000 kg and have a length of 12 to 16 m and a diameter of 3.6 to 4 m. The basic LST elements (Fig. 1) are the Optical Telescope Assembly (OTA), the Scientific Instruments (SI), and the Support Systems Module (SSM). The most important optical element in the OTA will be a diffraction-limited primary mirror approximately 3 m in diameter. The potential scientific instruments include a diffraction-limited camera and a low and a high dispersion spectrograph. All support systems such as control actuators, electronics, the power unit, and the data transmission assembly are combined in the SSM. Solar panels will supply the electrical power to the LST. The spacecraft will orbit earth at an altitude of 600 to 800 km at an inclination of 28.5 deg. Further details are given in Reference 1 and an LST briefing to industry.*

One of the main problems in the early LST system analysis has been the image motion stabilization to within 0.005 arc sec rms necessary to achieve the maximum benefit from the diffraction-limited telescope. The primary stabilization approaches are the secondary mirror control with the spacecraft stabilized to ±1 arc sec and the fine body pointing of the entire spacecraft to 0.005 arc sec rms. Several studies have been concerned with the body pointing. Johns [2] has shown that performance of about ±0.5 arc sec is achievable using single-gimbal control moment gyros only. Hartter et al. [3] have studied a control system with double-gimbal control moment gyros and reaction wheels. Under the influence of the gravity-gradient disturbance torques, a pointing accuracy of ±0.001 arc sec was found. Proise [4] has investigated a control system with reaction wheels only. Including gravity-gradient torques and sensor noise, a minimum pointing error of 0.0037 arc sec rms was reported, indicating the important impact of sensor noise. Thus, it has been shown that performance comparable to the required 0.005 arc sec rms might be achievable. However, critical aspects remain, e.g., gyro and reaction wheel vibrations, bending modes, nonlinearities, etc., all of which may degrade the pointing stability.

* LST Briefing to Industry on Phase A Results, Program Development Directorate, Marshall Space Flight Center, Huntsville, Ala., November 1972.

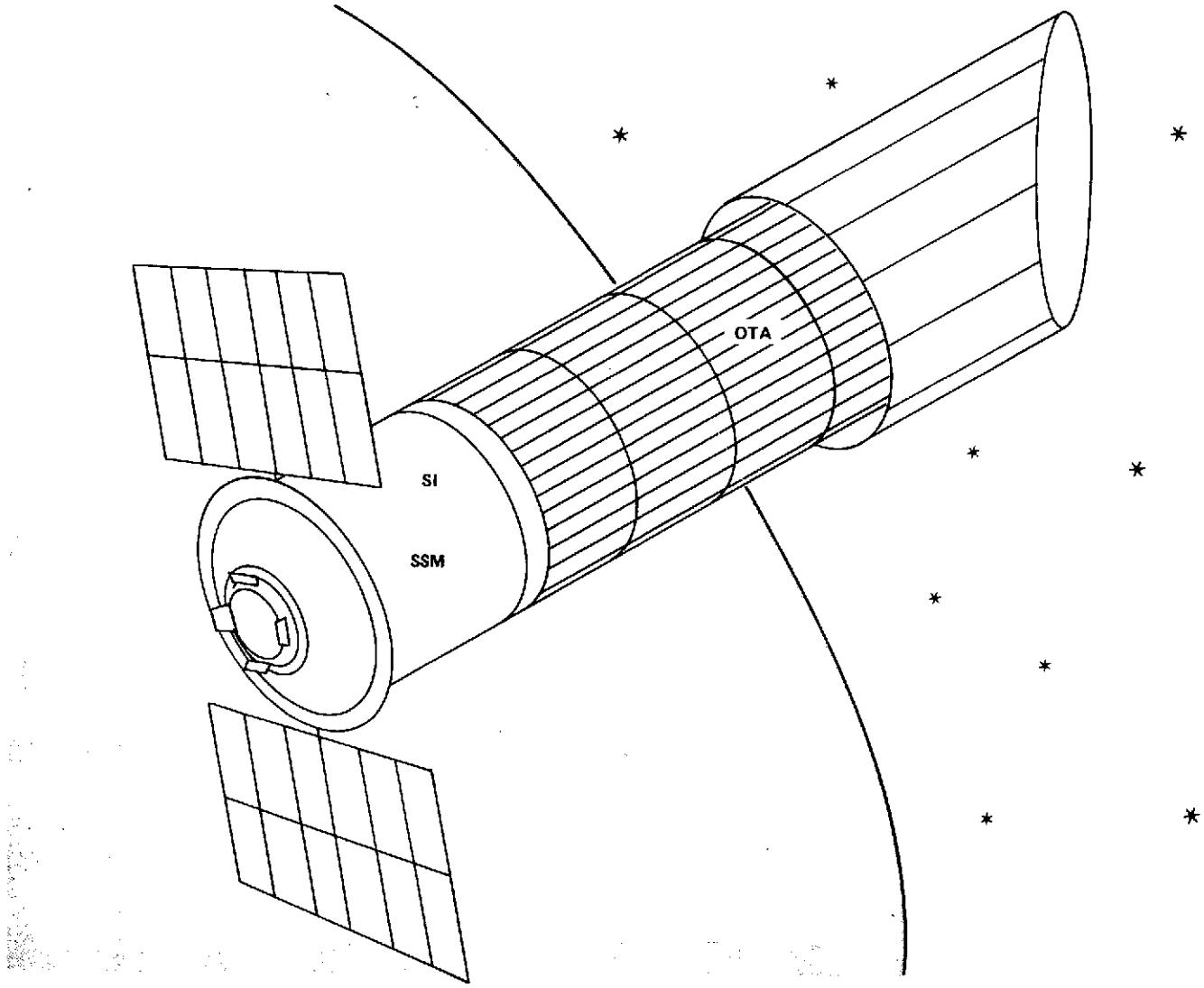

Figure 1. LST spacecraft configuration.

This report is divided into six major sections. The first section contains a description of the LST model and the general guidelines and assumptions. In the second section, the control system design philosophy is discussed, and a controller is constructed for the complete cancellation of the disturbance torques. The third section deals with the asymptotic stability and the transient analysis of the control system characterized by the impulse response. In the fourth section, the steady-state response of the system to noise excitations is investigated. The steady-state standard deviation (rms) of the LST attitude motion is optimized with respect to the system's characteristic frequency featuring the Disturbance Accommodation Standard deviation Optimal Controller (DASOC). In the fifth section, the sensitivity of the DASOC caused by variations in disturbance frequency is found from the corresponding frequency response. Finally, in the sixth section, the pointing stability achievable by the DASOC is compared with the results, using a Proportional Controller (PC), a Proportional Integral Controller (PIC), and a Proportional Integral Squared Controller (PI^2C). In addition to the factor of 3 improvement of the PI^2C over the PC, the DASOC offers a possible factor of 30 improvement in pointing stability. Furthermore, the corresponding characteristic frequency will be far below the first bending mode of the LST structure. The report appendix summarizes the spectral density analysis and the covariance analysis of linear differential equations driven by white noise. In this report, the covariance analysis will be used primarily.

DESCRIPTION OF THE LST MODEL

The LST (Fig. 2) consists primarily of the OTA, the SI, and the SSM. The LST spacecraft has a nearly cylindrical, beam-like shape. The principal axes frame S , with its origin at the center of mass, is defined as follows: The x_S-axis corresponds to the telescope axis, the y_S-axis is located along the solar wing axis, and the z_S-axis completes the orthogonal frame. The fine guidance system will maintain the frame S close to a given inertial reference frame I . Thus, the transformation matrix between frame I and frame S reads as

$$IS_A = \begin{bmatrix} 1 & -\psi & \theta \\ \psi & 1 & -\phi \\ -\theta & \phi & 1 \end{bmatrix}, \quad \phi \ll 1 , \ \theta \ll 1 , \ \psi \ll 1 \tag{1}$$

where ϕ is the roll angle, θ the pitch angle, and ψ the yaw angle. High accuracy is required in the pitch and yaw motion since these motions affect the pointing stability of the telescope axis. The angular velocity vector $\underline{\omega}$ of the LST relative to the frame I is

$$\underline{\omega} = [\dot{\phi} \ \dot{\theta} \ \dot{\psi}]^T \tag{2}$$

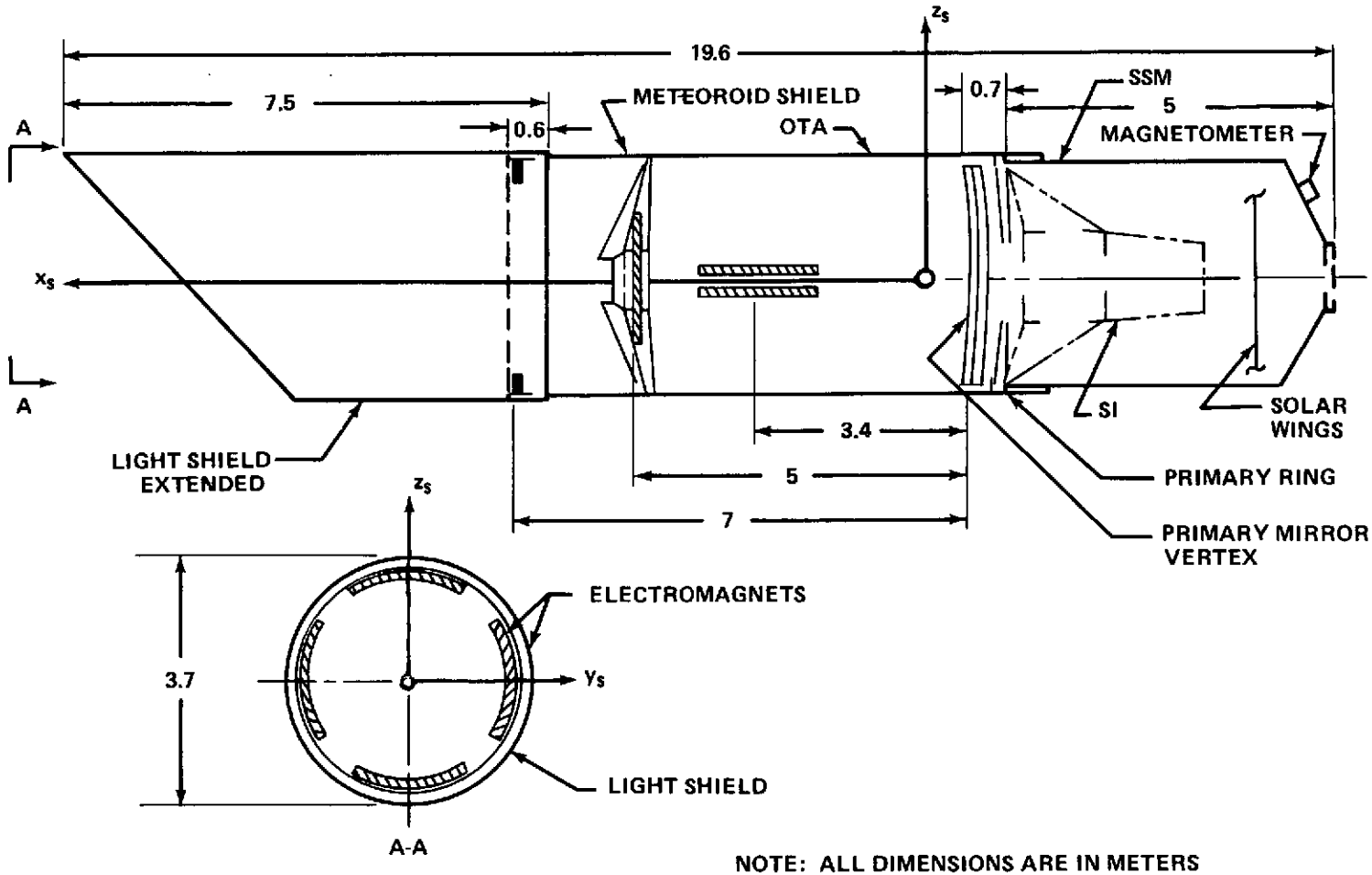

Figure 2. Basic LST elements and principal axes.

The LST will be assumed to be a rigid body; this is a legitimate assumption for the control system analysis because the structural frequencies are considerably higher than those of the control system. The reference cited in the footnote on page 1, for instance, indicates that the bending frequencies of the LST are all greater than 5.7 rad/sec. On the other hand, the characteristic frequency of the fine guidance system will be less than 0.1 rad/sec. Thus, the rigid body model will be a reliable approximation. The inertia tensor $\underline{I}$ of the LST is given by

$$\underline{I} = \begin{bmatrix} I_x & 0 & 0 \\ 0 & I_y & 0 \\ 0 & 0 & I_z \end{bmatrix} \tag{3}$$

where $I_x = 14\,656$ kgm^2, $I_y = 91\,772$ kgm^2, and $I_z = 95\,027$ kgm^2 in the on-orbit configuration with extended light shield and solar wings. The corresponding mass totals 9380 kg.

Within the SSM, there will be three symmetric reaction wheels with inertia tensors

$$\underline{I}_1 = \begin{bmatrix} I_{1x} & 0 & 0 \\ 0 & I_{1y} & 0 \\ 0 & 0 & I_{1y} \end{bmatrix}, \quad \underline{I}_2 = \begin{bmatrix} I_{2z} & 0 & 0 \\ 0 & I_{2y} & 0 \\ 0 & 0 & I_{2z} \end{bmatrix}, \quad \underline{I}_3 = \begin{bmatrix} I_{3x} & 0 & 0 \\ 0 & I_{3x} & 0 \\ 0 & 0 & I_{3z} \end{bmatrix} \tag{4}$$

and the angular velocities relative to frame S:

$$\underline{\omega}_1 = \begin{bmatrix} \nu_1 \\ 0 \\ 0 \end{bmatrix}, \quad \underline{\omega}_2 = \begin{bmatrix} 0 \\ \nu_2 \\ 0 \end{bmatrix}, \quad \underline{\omega}_3 = \begin{bmatrix} 0 \\ 0 \\ \nu_3 \end{bmatrix} \tag{5}$$

The reaction wheels, then, are mounted parallel to the axes x_S, y_S, z_S, respectively.

The spacecraft's equation of motion follows now from the Euler equations, given in Reference 5.

$$\underline{I} \cdot \dot{\underline{\omega}} + \underline{\omega} \times \underline{I} \cdot \underline{\omega} + \sum_{i=1}^{3} [\underline{\omega} \times \underline{\omega}_i \, \mathrm{tr}\, \underline{I}_i + 2\underline{\omega}_i \times \underline{I}_i \cdot \underline{\omega}$$

$$+ \underline{I}_i \cdot \dot{\underline{\omega}}_i + \underline{\omega}_i \times \underline{I}_i \cdot \underline{\omega}_i] = \underline{M} \qquad (6)$$

and

$$\underline{I}_i \cdot \dot{\underline{\omega}} + \underline{\omega} \times \underline{I}_i \cdot \underline{\omega} + \underline{\omega} \times \underline{\omega}_i \, \mathrm{tr}\, \underline{I}_i + 2\underline{\omega}_i \times \underline{I}_i \cdot \underline{\omega}$$

$$+ \underline{I}_i \cdot \dot{\underline{\omega}}_i + \underline{\omega}_i \times \underline{I}_i \cdot \underline{\omega}_i = \underline{M}_i \quad , \quad i = 1(1)3 \quad , \qquad (7)$$

where $\underline{M}$ is the external torque acting on the LST and $\underline{M}_i$ is the internal torque on the reaction wheels. Assuming small motions $\phi \ll 1$, $\theta \ll 1$, $\psi \ll 1$ and small reaction wheels $I_{ix} \ll I_x$, $I_{2y} \ll I_y$, $I_{3z} \ll I_z$, as well as the fact that the reaction wheels have one degree of freedom only, the following scalar equations are obtained from the vector equations (1) through (7):

$$I_x \ddot{\phi} + I_{1x} \dot{\nu}_1 = M_x \quad , \qquad (8)$$

$$I_y \ddot{\theta} + I_{2y} \dot{\nu}_2 = M_y \quad , \qquad (9)$$

$$I_z \ddot{\psi} + I_{3z} \dot{\nu}_3 = M_z \quad , \qquad (10)$$

$$I_{1x} \dot{\nu}_1 = M_{1x} \quad , \qquad (11)$$

$$I_{2y} \dot{\nu}_2 = M_{2y} \quad , \qquad (12)$$

and

$$I_{3z}\dot{\nu}_3 = M_{3z} \quad . \tag{13}$$

Clearly, these are three decoupled sets of equations and thus only a single axis analysis is necessary. Because of the high accuracy pointing requirements on the telescope axis, the pitch motion is chosen.

The internal torque, M_{2y}, can be written as

$$M_{2y} = M_{delay} + M_{drive} \tag{14}$$

where

$$M_{delay} = -d_0\nu_2 \tag{15}$$

is some delaying torque, e.g., viscous friction, and M_{drive} is the driving motor torque, M_{drive}, which is a linear function of the control variable u and compensates for the delaying torque M_{delay}, has the form:

$$M_{drive} = d_0\nu_2 - ku \quad . \tag{16}$$

Thus, from equations (9), (12), and (14) through (16), it follows that

$$I_y\ddot{\theta} = ku + M_y \quad . \tag{17}$$

In equation (17), the external torques M_y are not specified; they depend on the external environment in space. The maximum values of the respective external torques are given in Reference 1:

Gravity-gradient	0.2200 N-m
Magnetic	0.0500 N-m

Aerodynamic	0.0001 N-m
Solar pressure	0.0004 N-m

Clearly, the gravity-gradient and the magnetic torques are the significant disturbance torques, while the aerodynamic and the solar pressure torques are negligible.

The gravity-gradient torque acting on the LST spacecraft in a circular orbit with twice orbital rate ω reads as

$$\underline{M}_g = \frac{3}{4}\omega^2 \underline{e}_v \times \underline{I} \cdot \underline{e}_v \tag{18}$$

where $\underline{e}_v$ is the unit vector in the direction of the orbital radius vector. In the inertial frame O, Figure 3, $\underline{e}_v$ is

$${}_o\underline{e}_v = (\cos i \sin\tau \quad \sin i \sin\tau \quad \cos\tau)^T \tag{19}$$

where i is the orbital inclination and τ an angle locating the vehicle in orbit. The transformation matrix between frame O and the reference frame I is the constant matrix

$$OI_A = \begin{bmatrix} a_{11} & a_{12} & a_{13} \\ a_{21} & a_{22} & a_{23} \\ a_{31} & a_{32} & a_{33} \end{bmatrix} \tag{20}$$

Applying the transformation matrices (1) and (20) to the vertical vector (19), one obtains in frame S with $\phi \ll 1$, $\theta \ll 1$, $\psi \ll 1$:

$$\underline{e}_v = {}^{SI}_{A}\ {}^{IO}_{A}\ {}_o\underline{e}_v = \begin{bmatrix} a_{11}\cos i \sin\tau + a_{21}\sin i \sin\tau + a_{31}\cos\tau \\ a_{12}\cos i \sin\tau + a_{22}\sin i \sin\tau + a_{32}\cos\tau \\ a_{13}\cos i \sin\tau + a_{23}\sin i \sin\tau + a_{33}\cos\tau \end{bmatrix} . \tag{21}$$

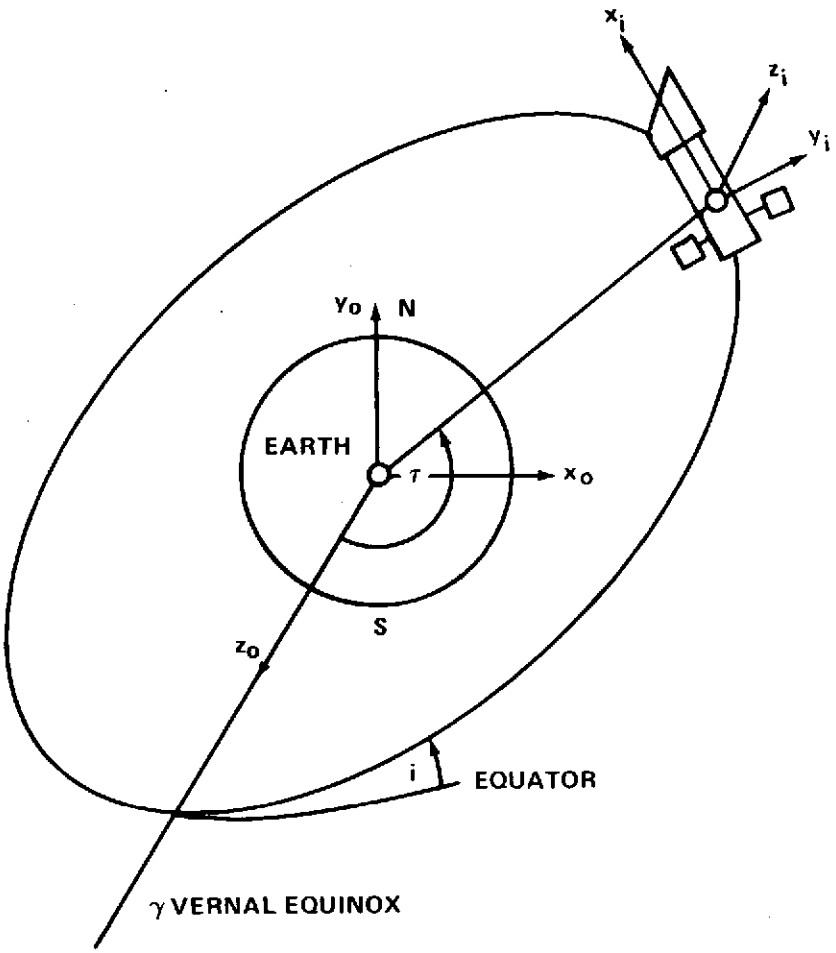

Figure 3. LST orbit and inertial frames.

Using equations (3) and (21), the gravity-gradient torque (18) can be written

$$\underline{M}_g = \frac{3\omega^2}{8} \begin{bmatrix} (I_z - I_y)(g_{x1} + g_{x2} \cos 2\tau) \\ (I_x - I_z)(g_{y1} + g_{y2} \cos 2\tau) \\ (I_y - I_x)(g_{z1} + g_{z2} \cos 2\tau) \end{bmatrix} \tag{22}$$

where $g_{xi} \leqslant 1$, $g_{yi} \leqslant 1$, $g_{zi} \leqslant 1$, $i = 1, 2$, are introduced as convenient abbreviations.

The magnetic torque acting on the LST is

$$\underline{M}_m = \underline{m} \times \underline{B} \tag{23}$$

where $\underline{m}$ is the LST dipole moment and $\underline{B}$ is the earth's magnetic field intensity. The dipole moment of the LST is composed of a constant moment inherent in the structure and a nonconstant moment generated by desaturation magnets. In each case, the dipole moment will usually be fixed within the LST and may be piecewise constant in time, depending on the desaturation procedure. The dipole moment is characterized by a unit vector $\underline{e}_m$ and the magnitude m_o:

$$\underline{m} = m_o \cdot \underline{e}_m \quad . \tag{24}$$

The magnetic field intensity is, according to McElvain [6], in frame O with the y_o-axis approximately corresponding to the earth's magnetic axis:

$$_o\underline{B} = 3B_o \begin{bmatrix} \sin i \cos i \sin^2 \tau \\ \sin^2 i \sin^2 \tau - 1/3 \\ \sin i \sin \tau \cos \tau \end{bmatrix} \quad . \tag{25}$$

Using the equations (1) and (20), one obtains from equations (23) through (25) the magnetic torque in frame S:

$$\underline{M}_m = 3m_oB_o \begin{bmatrix} h_{x1} + h_{x2} \cos 2\tau \\ h_{y1} + h_{y2} \cos 2\tau \\ h_{z1} + h_{z2} \cos 2\tau \end{bmatrix} \tag{26}$$

where h_{xi}, h_{yi}, h_{zi}, $i = 1, 2$, depend on the unit vector $\underline{e}_m$, the transformation matrices, ^{OI}A, ^{IS}A, and the orbital inclination i.

The small aerodynamic and solar pressure torque may be modeled by a random torque acting on the LST:

$$\underline{M}_{as} = [M_{asx}(t)\ M_{asy}(t)\ M_{asz}(t)]^T \quad . \tag{27}$$

This random torque will be a stationary white noise process with zero mean and constant spectral density.

The external torque M_y acting on the pitch axis can now be found from equations (22), (26), and (27) as

$$M_y = I_y[\beta + \gamma \cos(\omega t + \chi) + s(t)] \tag{28}$$

where

$$\beta = \frac{3\omega^2}{8} \frac{I_x - I_z}{I_y} g_{y1} + \frac{3m_0 B_0}{I_y} h_{y1} \quad , \tag{29}$$

$$\gamma = \frac{3\omega^2}{8} \frac{I_x - I_z}{I_y} g_{y2} + \frac{3m_0 B_0}{I_y} h_{y2} \quad , \tag{30}$$

$$\omega t + \chi = 2\tau \quad , \tag{31}$$

and

$$s(t) = \frac{M_{asy}(t)}{I_y} \sim (0, q) \quad . \tag{32}$$

In equation (31), the twice orbital rate ω appears again together with some phase angle χ. The white noise process s(t) used in equation (32) is characterized by zero mean and spectral density q. The coefficients β, γ, and the phase angle χ need not be specified, because they will be generated on-line in the controller.

The only restriction on β , γ , and χ is that they are constant or, at most, varying from time to time. The twice orbital rate is approximately $\omega = 2 \times 10^{-3}$ rad/sec for an altitude of 800 km and the spectral density, q , is estimated to $q = 1 \times 10^{-12}$ arc sec^2/sec^3 . Finally, one obtains from equations (17) and (28) the system equation,

$$\ddot{\theta} = bu + \beta + \gamma \cos(\omega t + \chi) + s \quad , \tag{33}$$

where

$$b = k/I_y \quad .$$

The fine guidance sensor, part of the SI and shown in Figure 4, consists of two image dissectors which develop error signals as a function of the vehicle attitude motion. However, the sensor signals are disturbed by electronic noise generated primarily in the photocathode tube. The sensor signal y corresponding to the pitch motion θ can be represented by

$$y = \theta + v \quad , \quad v \sim (0 , r) \tag{34}$$

where the sensor noise v will be a stationary white noise process with zero mean and spectral density r . This spectral density r has been estimated by Kolsman Instruments, as shown in Reference 4. It is a function of the brightness of the guide star (m_v) and the amount of the guide star offset from the telescope pointing axis (ρ) . The spectral density can be expressed mathematically as

$$r = 9.959 \times 10^{-18} \quad (2.51)^{m_v} \quad \rho^{5.48} \tag{35}$$

where r is given in arc sec^2 seconds and ρ in arc minutes.

For a typical guide star of magnitude $m_v = 12$ and a guide star offset $\rho = 20$ arc min, the spectral density turns out to be $r = 8.394 \times 10^{-6}$ arc sec^2 sec.

Finally, the description of the LST model will be represented by the linear, time-invariant system,

$$\dot{x} = Ax + Bu + Fw + Gs \tag{36}$$

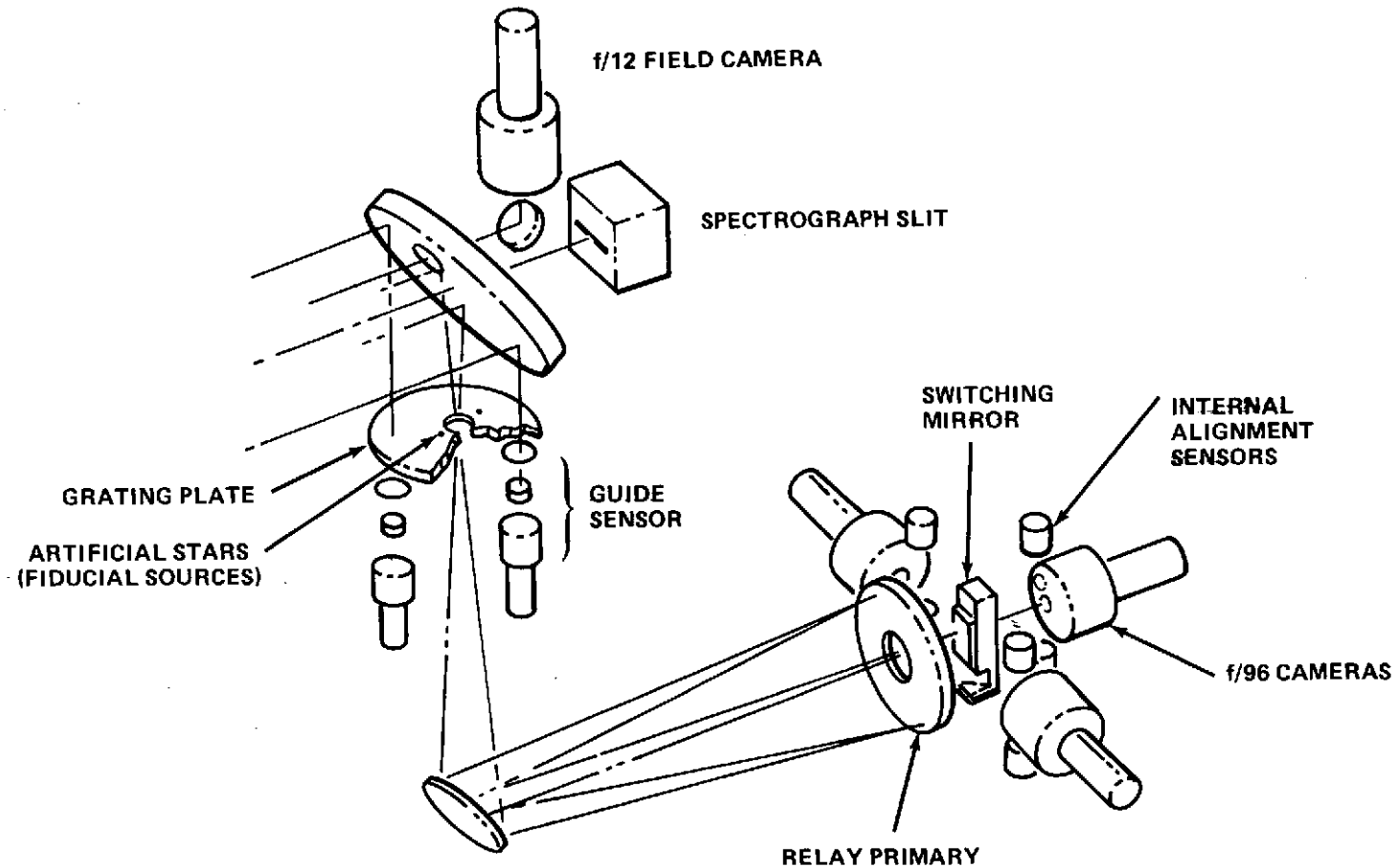

Figure 4. Fine guidance sensor.

and

$$y = Cx + v \quad , \tag{37}$$

using the state vector

$$x = [\theta \ \dot{\theta}]^T \tag{38}$$

and the deterministic, scalar disturbance

$$w = \beta + \gamma \cos(\omega t + \chi) \quad . \tag{39}$$

The matrices A, B, C, F, G are easily obtained from equations (33), (34), (38) and (39):

$$A = \begin{bmatrix} 0 & 1 \\ 0 & 0 \end{bmatrix} , \qquad B = \begin{bmatrix} 0 \\ b \end{bmatrix} , \qquad C = [1 \quad 0] \ ,$$

$$F = \begin{bmatrix} 0 \\ 1 \end{bmatrix} , \qquad G = \begin{bmatrix} 0 \\ 1 \end{bmatrix} \quad . \tag{40}$$

A block diagram of the LST model is given in Figure 5.

DISTURBANCE ACCOMMODATION CONTROL SYSTEM DESIGN

For the LST modeled by the system (36) and (37), a controller must be designed. The design philosophy follows immediately from some principal phenomena found by Proise [4]. Using a lead network and a PC for the system (36) and (37), the LST pointing stability depends on the characteristic frequency α of the closed-loop control system (Fig. 6). With an increasing characteristic frequency, the response to the disturbance torques decreases whereas the response to the sensor noise increases. Thus, a unique optimal pointing stability can be found. For a further improvement of the

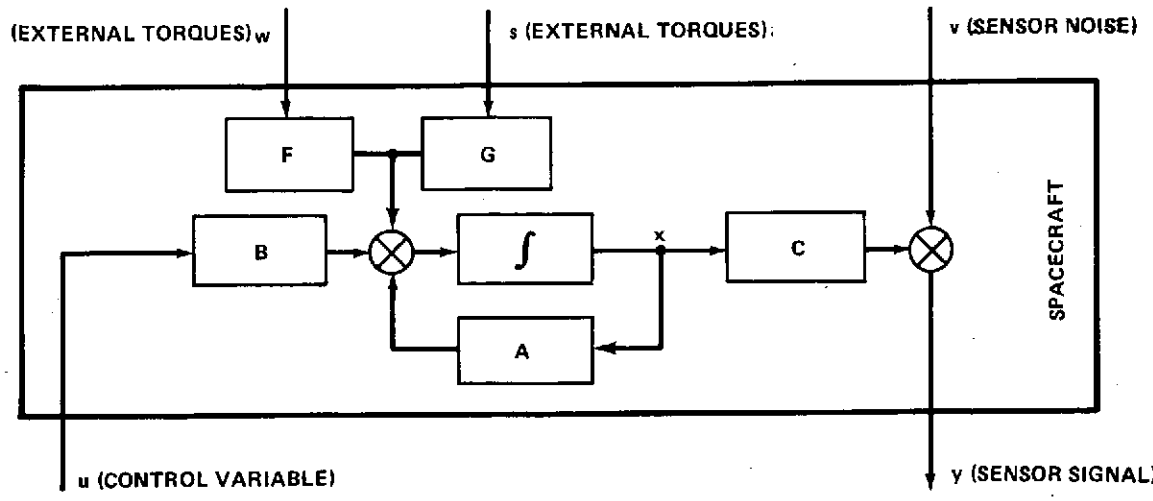

Figure 5. Block diagram of the LST model.

pointing stability, either the response to the disturbance torques or the response to the sensor noise has to be reduced by more sophisticated controllers. Because the sensor noise is a stochastic process, there is very little prospect for getting a large improvement by a different controller. On the other hand, the disturbance torques are essentially known, deterministic functions which might be cancelled out by a well-matched controller. A reduction of the disturbance torque response offers a decrease in the characteristic frequency, which produces the additional advantage of reducing the interaction of the pointing and structural bending motion. In Reference 4, Proise has substituted for the PC the PIC and PI^2C, resulting in a factor of 3 improvement in pointing stability and a factor of 9 reduction in optimal characteristic frequency. Principally, the PIC or PI^2C, are well matched for the cancellation of constant or ramp disturbances, respectively, but they fit only approximately for sinusoidal disturbances. Therefore, a more sophisticated controller will now be designed using the accommodation of external disturbances in linear control systems recently developed by Johnson [7, 8, 9] and Davison. [10] The fundamental idea of the disturbance accommodation is the modeling of the disturbance function by differential equations. For this purpose, the shape of the waveform of the expected disturbance function must be known. This means, in general, that only the frequencies in the Fourier expansion of the disturbance function, and not the amplitudes and phase angles, give the essential and necessary information for the disturbance modeling. The disturbance differential equations are then used to complete the system differential equations, and a common observer is used for the estimation of state and disturbance. The state estimation is fed back by the regulator to obtain stability and satisfactory transient response, and the disturbance estimation is fed back by the accommodator to cancel out the disturbances.

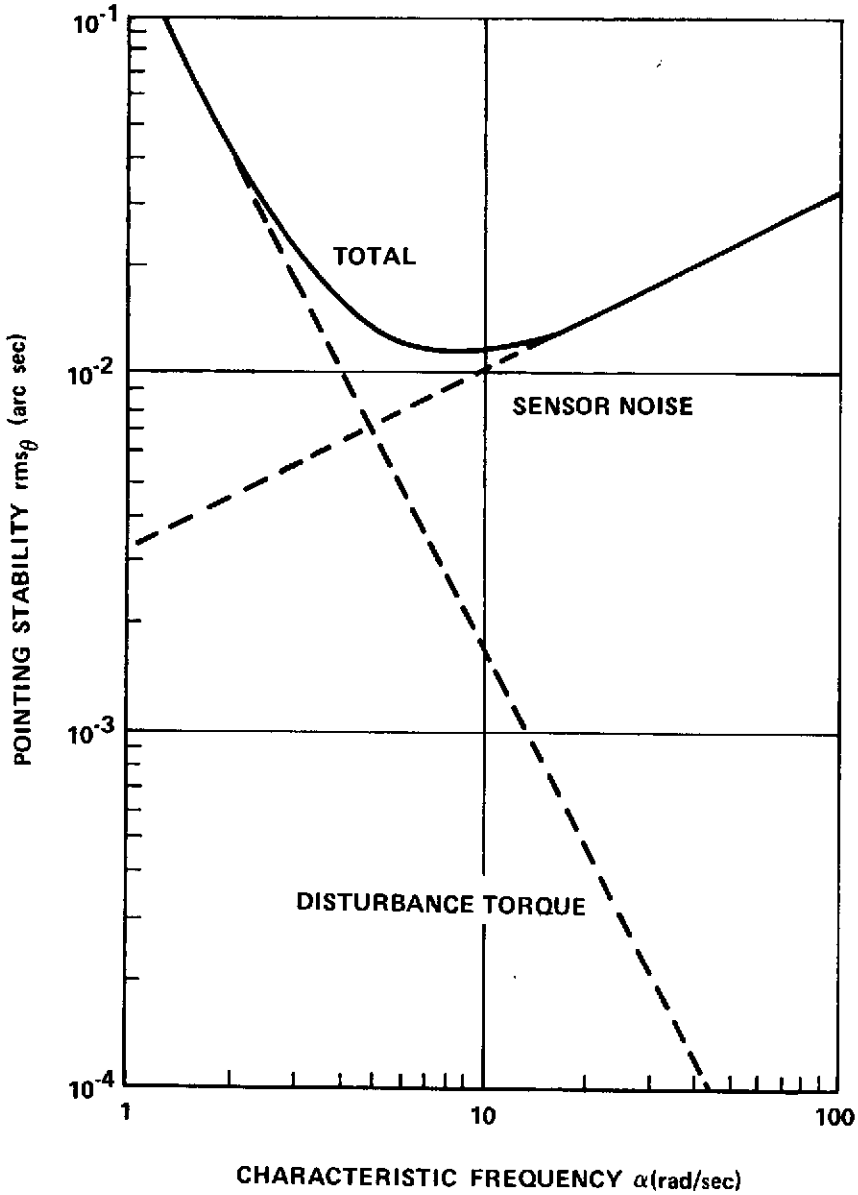

Figure 6. Response with proportional controller.

For the linear system represented as

$$\dot{x} = Ax + Bu + Fw \tag{41}$$

$$y = Cx \tag{42}$$

and the disturbance model as

$$\dot{z} = Dz \tag{43}$$

$$w = Hz \quad , \tag{44}$$

Johnson has used the following control law,

$$u = u_c + u_r \quad , \tag{45}$$

with the counteraction mode,

$$u_c = -\Gamma\hat{w} \quad , \tag{46}$$

and the regulator mode,

$$u_r = -L\hat{x} \quad . \tag{47}$$

A cancellation or counteracting control u_c exists if

$$F = B\Gamma \tag{48}$$

for some matrix Γ. The estimations $\hat{x}$, $\hat{z}$ can be obtained from the observer-accommodator

$$\begin{bmatrix} \dot{\hat{x}} \\ \dot{\hat{z}} \end{bmatrix} = \left[\begin{array}{c|c} A-BL + K_1C & 0 \\ \hline K_2C & D \end{array}\right] \begin{bmatrix} \hat{x} \\ \hat{z} \end{bmatrix} - \begin{bmatrix} K_1 \\ K_2 \end{bmatrix} y \quad . \tag{49}$$

The controller parameters are the elements of the matrices K_1 , K_2 , and L . Johnson recommends that a fast observer be implemented by K_1 and K_2 and an optimal

regulator by L. However, these recommendations cannot be used for the LST because a fast observer would amplify the sensor noise which was not considered in Johnson's system (41) and (42). Davison's approach to the disturbance accommodation is not as general as Johnson's approach. Davison uses the complete state for the feedback in the regulator loop which is not available for the LST. Furthermore, Davison guarantees only that there will be no output response for an external disturbance input, leaving the possibility of an internal steady-state motion which might excite structural vibrations. Therefore, Johnson's approach will be used here.

First of all, the differential equations modeling the deterministic disturbance given in equation (39) must be added to the system equations (36) and (37). Since the disturbance is a linear combination of a constant and a sinusoidal term, the following disturbance state equations are used:

$$\dot{z}_1 = 0 \tag{50}$$

$$\dot{z}_2 = \omega z_3 \tag{51}$$

$$\dot{z}_3 = -\omega z_2 \quad . \tag{52}$$

With these equations, the matrices in the vector equations (43) and (44) read as

$$D = \begin{bmatrix} 0 & 0 & 0 \\ 0 & 0 & \omega \\ 0 & -\omega & 0 \end{bmatrix}, \quad H = [1 \;\; 1 \;\; 0] \quad . \tag{53}$$

Further, the controller parameters will be specified as:

regulator parameter matrix,

$$L = [c \;\; d] \quad ; \tag{54}$$

observer parameter matrix,

$$K_1 = [k_1 \;\; k_2]^T \quad ; \tag{55}$$

accommodator parameter matrix,

$$K_2 = [k_3 \;\; k_4 \;\; k_5]^T \quad . \tag{56}$$

Now all the matrices of the controller represented by equations (45) through (49) are specified. Combined with this controller, the open-loop system (36) and (37) results in the following closed-loop system:

$$\dot{x} = Ax - BL\hat{x} - FH\hat{z} + Fw + Gs \quad , \tag{57}$$

$$\dot{\hat{x}} = (A - BL + K_1 C)\,\hat{x} - K_1 Cx - K_1 v \quad , \tag{58}$$

$$\dot{\hat{z}} = D\hat{z} + K_2 C\hat{x} - K_2 Cx - K_2 v \quad . \tag{59}$$

A block diagram of the closed-loop fine pointing system is shown in Figure 7, representing the three different loops of the controller:

1. The observer for reconstruction of the complete state
2. The regulator for the state feedback
3. The accommodator for cancellation of the disturbance torques.

Equations (57) through (59) can be condensed by using a generalized state vector $X = [x^T \hat{x}^T \hat{z}^T]^T$, a generalized deterministic disturbance $W = w$, and a generalized noise excitation $V = [s\ v]^T$:

$$\dot{X} = \bar{A}X + \bar{F}W + \bar{G}V \quad . \tag{60}$$

The matrices $\bar{A}$, $\bar{F}$, and $\bar{G}$ found from equations (40) and (53) through (59) are listed in Table 1.

The initial state vector of the differential equation (60) is given by

$$X(O) = X_o \tag{61}$$

and will be introduced as a Gaussian random vector,

$$X_o \sim (\bar{X}_o \ , \ P_o) \quad , \tag{62}$$

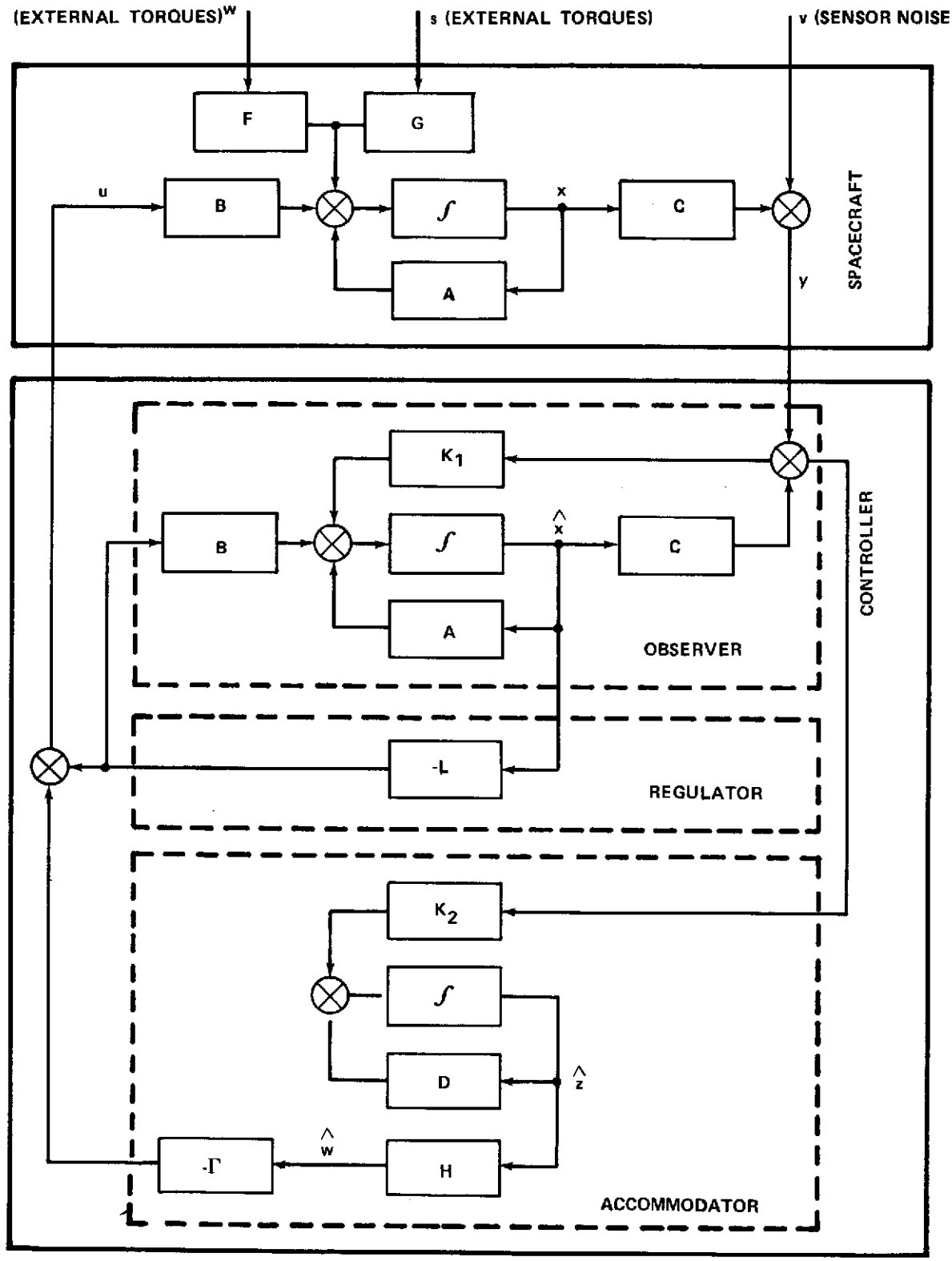

Figure 7. Block diagram of the fine pointing system.

TABLE 1. FINE POINTING SYSTEM MATRICES DEPENDING ON THE FREE PARAMETERS

$$\bar{A} = \begin{bmatrix} 0 & 1 & 0 & 0 & 0 & 0 & 0 \\ 0 & 0 & -bc & -bd & -1 & -1 & 0 \\ -k_1 & 0 & k_1 & 1 & 0 & 0 & 0 \\ -k_2 & 0 & k_2\text{-}bc & -bd & 0 & 0 & 0 \\ -k_3 & 0 & k_3 & 0 & 0 & 0 & 0 \\ -k_4 & 0 & k_4 & 0 & 0 & 0 & \omega \\ -k_5 & 0 & k_5 & 0 & 0 & -\omega & 0 \end{bmatrix} \qquad \bar{F} = \begin{bmatrix} 0 \\ 1 \\ 0 \\ 0 \\ 0 \\ 0 \\ 0 \end{bmatrix} \qquad \bar{G} = \begin{bmatrix} 0 & 0 \\ 1 & 0 \\ 0 & -k_1 \\ 0 & -k_2 \\ 0 & -k_3 \\ 0 & -k_4 \\ 0 & -k_5 \end{bmatrix}$$

where $\bar{X}_0$ is the mean vector, and P_0 is the covariance matrix. If no initial information on X_0 is available, $\bar{X}_0 = 0$ and $P_0 = E$ are useful assumptions. Here E is the unit matrix. The deterministic disturbance remains unchanged and follows immediately from equation (39) as

$$W = \beta + \gamma \cos(\omega t + \chi) \quad . \tag{63}$$

The noise excitation vector is characterized by the white noise process

$$V \sim (O , S) , \qquad S = \begin{bmatrix} q & O \\ O & r \end{bmatrix} , \tag{64}$$

which is composed of the scalar processes (32) and (34).

The existence of the controller represented by equations (45) through (49) depends on the controllability of the system (41), as well as on the observability of the system (41) through (44) and the cancellation condition (48). All three conditions will now be checked, using the matrices (40) and (53). The controllability matrix has the full rank,

$$\text{rank } [B \vdots AB] = \text{rank} \begin{bmatrix} 0 & b \\ b & 0 \end{bmatrix} = 2 , \tag{65}$$

proving controllability. The observability matrix corresponding to the system and disturbance state vector $[x^T z^T]^T$ has the full rank,

$$\text{rank} \left[\begin{bmatrix} C^T \\ O \end{bmatrix} \vdots \begin{bmatrix} A & FH \\ O & D \end{bmatrix}^T \begin{bmatrix} C^T \\ O \end{bmatrix} \vdots \cdots \vdots \begin{bmatrix} A & FH \\ O & D \end{bmatrix}^{T^{(n-1)}} \begin{bmatrix} C^T \\ O \end{bmatrix} \right]$$

$$= \text{rank} \begin{bmatrix} 1 & 0 & 0 & 0 & 0 \\ 0 & 1 & 0 & 0 & 0 \\ 0 & 0 & 1 & 0 & 0 \\ 0 & 0 & 1 & 0 & -\omega^2 \\ 0 & 0 & 0 & -\omega & 0 \end{bmatrix} = 5 \quad , \tag{66}$$

proving the observability of the system state and disturbance state. The exponent, n , is the order of the system defined by equations (41) and (43). The matrix Γ follows as

$$\Gamma = \frac{1}{b} \quad , \tag{67}$$

proving the counteraction mode.

So far the controller has been designed and its existence has been proved. Seven parameters have been found in the matrices (54) through (56) which are free with respect to the disturbance accommodation mode. These parameters will be constrained by the stability conditions and can be optimized with respect to the transient response and/or the noise response. The steady-state response to the deterministic disturbance (63) is identically zero as a result of the disturbance accommodation system design.

STABILITY AND TRANSIENT RESPONSE

The asymptotic stability and the transient response of the undisturbed closed-loop system depend only on the homogeneous part of the differential equation (60), which is

$$\dot{X} = \bar{A}X \quad , \quad X(0) = X_0 \quad . \tag{68}$$

The asymptotic stability will be checked by applying the Liénard-Chipart stability conditions on the characteristic equation,

$$\det(\lambda E - \bar{A}) = \lambda^7 + a_1\lambda^6 + a_2\lambda^5 + a_3\lambda^4 + a_4\lambda^3 + a_5\lambda^2 + a_6\lambda + a_7 = 0 \, . \tag{69}$$

These conditions, according to Porter [11] are simply

$$a_7 > 0 \ , \ a_5 > 0 \ , \ a_3 > 0 \ , \ a_1 > 0 \ , \ H_6 > 0 \ , \ H_4 > 0 \ , \text{ and } H_2 > 0 \tag{70}$$

where H_i is the ith principal minor of the Hurwitz matrix

$$H = \begin{bmatrix} a_1 & 1 & 0 & 0 & 0 & 0 & 0 \\ a_3 & a_2 & a_1 & 1 & 0 & 0 & 0 \\ a_5 & a_4 & a_3 & a_2 & a_1 & 1 & 0 \\ a_7 & a_6 & a_5 & a_4 & a_3 & a_2 & a_1 \\ 0 & 0 & a_7 & a_6 & a_5 & a_4 & a_3 \\ 0 & 0 & 0 & 0 & a_7 & a_6 & a_5 \\ 0 & 0 & 0 & 0 & 0 & 0 & a_7 \end{bmatrix} \tag{71}$$

The evaluation of the characteristic equation (69) using $\bar{A}$ from Table 1 results in

$$\det(\lambda E - \bar{A}) = (\lambda^2 + bd\lambda + bc)[\lambda^5 - k_1\lambda^4 + (\omega^2 - k_2)\lambda^3$$

$$- (k_1\omega^2 + k_3 + k_4)\lambda^2 - \omega(k_2\omega + k_5)\lambda - \omega^2 k_3] = 0 \, . \tag{72}$$

Clearly, the two eigenvalues of the system associated with the regulator and the five associated with the observer with accommodator are completely separated. Therefore, the stability conditions (70) can be applied to the second-order and the fifth-order characteristic equation within the seventh-order characteristic equation (72) separately. The results are listed in Table 2.

TABLE 2. STABILITY CONDITIONS DEPENDING ON THE FREE PARAMETERS

NO.	STABILITY CONDITION
1	$bc > 0$
2	$bd > 0$
3	$k_1 < 0$
4	$k_3 < 0$
5	$k_1\omega^2 + k_3 + k_4 < 0$
6	$k_1k_2 + k_3 + k_4 > 0$
7	$\{(k_1k_2 + k_3 + k_4)k_2 + (k_1k_2 + k_3)\omega^2\}k_4\omega$ $+\{(k_1k_2 + k_3 + k_4)(k_3 + k_4) - (k_1k_2 + k_3 - k_4)k_1\omega^2\}k_5$ $-k_1^2k_5^2\omega > 0$

The seven free parameters $c, d, k_1, k_2, \ldots k_5$ are now constrained because of the stability conditions of Table 2. But within these constraints they remain free and can be used to optimize the responses of the closed-loop system with respect to initial conditions or impulses and/or with respect to steady-state noise disturbances. Five different optimization approaches are listed as follows:

1. Nonoptimal transient response, wherein all seven free parameters can be used for optimization of the steady-state response.

2. Suboptimal transient response with two parameters optimal in the sense of a quadratic performance index (Johnson's approach of the optimal regulator). Then five parameters are left for the optimization of the steady-state response.

3. Suboptimal transient response with two additional parameters optimal in the sense of state estimation (optimal regulator and Kalman filter). Three parameters are left for the optimization of the steady-state response.

4. Suboptimal transient response with six parameters optimal in the sense of pole assignment (eigenvalues proportional to a characteristic frequency). One parameter can be used for the optimization of the steady-state response.

5. Optimal transient response using all seven parameters; nonoptimal steady-state response.

All optimizations, except the optimal regulator, Kalman filter, and pole assignment, are pure parameter optimizations, which must be done by computer search methods.

For the LST fine pointing system, the suboptimal transient response in the sense of pole assignment will be used so that interactions between pointing motion frequencies and bending frequencies will be minimized.

Clearly, the frequencies or the negative eigenvalues must be as small as possible from the interaction point of view. On the other hand, the negative eigenvalues have to be as large as possible to furnish a good degree of stability and a short settling time. Thus, an optimum will be a sevenfold negative real eigenvalue. The magnitude of this multiple eigenvalue has to be variable for the steady-state response optimization, and this variable magnitude will serve as the system's characteristic frequency.

The control system designed as described in the section, Disturbance Accommodation Control System Design, is completely controllable and completely observable. Therefore, the eigenvalues can be chosen arbitrarily, and they will be chosen optimally as a sevenfold eigenvalue

$$\lambda_i = -\alpha \quad , \quad i = 1(1)7 \quad , \tag{73}$$

where α is the sytem's characteristic frequency. The corresponding characteristic equation reads as

$$\begin{aligned} \det(\lambda E - \bar{A}) &= (\lambda + \alpha)^7 \\ &= (\lambda^2 + 2\alpha\lambda + \alpha^2)(\lambda^5 + 5\alpha\lambda^4 + 10\alpha^2\lambda^3 + 10\alpha^3\lambda^2 \\ &\quad + 5\alpha^4\lambda + \alpha^5) = 0 \quad . \end{aligned} \tag{74}$$

By comparison of the coefficients in equations (72) and (74), the seven free parameters are defined as follows:

$$c = \alpha^2/b \quad , \tag{75}$$

$$d = 2\alpha/b \quad , \tag{76}$$

$$k_1 = -5\alpha \quad , \tag{77}$$

$$k_2 = \omega^2 - 10\alpha^2 \quad , \tag{78}$$

$$k_3 = -\alpha^5/\omega^2 \quad , \tag{79}$$

$$k_4 = 5\omega^2\alpha - 10\alpha^3 + \alpha^5/\omega^2 \quad , \tag{80}$$

and

$$k_5 = -\omega^3 + 10\omega\alpha^2 - 5\alpha^4/\omega \quad . \tag{81}$$

Using the parameters (75) through (81) and Table 1, one obtains the matrices $\overline{A}$, $\overline{F}$, $\overline{G}$ of the closed-loop system, depending on the characteristic frequency α, rewritten in Table 3. The asymptotic stability of the closed-loop system is now guaranteed for all positive characteristic frequencies, $\alpha > 0$, following from the stability conditions in Table 2 or immediately from equation (73). A stability analysis is not required later.

OPTIMIZATION OF THE NOISE RESPONSE

The response of the closed-loop system to noise inputs depends on the stochastic part of differential equation (60), written as

$$\dot{X} = \overline{A}X + \overline{G}V \tag{82}$$

TABLE 3. FINE POINTING SYSTEM MATRICES DEPENDING ON THE CHARACTERISTIC FREQUENCY

$$\bar{A} = \begin{bmatrix} 0 & 1 & 0 & 0 & 0 & 0 & 0 \\ 0 & 0 & -a^2 & -2a & -1 & -1 & 0 \\ 5a & 0 & -5a & 1 & 0 & 0 & 0 \\ 10a^2-\omega^2 & 0 & 9a^2-\omega^2 & -2a & 0 & 0 & 0 \\ a^5/\omega^2 & 0 & -(a^5/\omega^2) & 0 & 0 & 0 & 0 \\ -k_4 & 0 & k_4 & 0 & 0 & 0 & \omega \\ -k_5 & 0 & k_5 & 0 & 0 & -\omega & 0 \end{bmatrix} \qquad \bar{F} = \begin{bmatrix} 0 \\ 1 \\ 0 \\ 0 \\ 0 \\ 0 \\ 0 \end{bmatrix} \qquad \bar{G} = \begin{bmatrix} 0 & 0 \\ 1 & 0 \\ 0 & 5a \\ 0 & 10a^2-\omega^2 \\ 0 & a^5/\omega^2 \\ 0 & -k_4 \\ 0 & -k_5 \end{bmatrix}$$

$$k_4 = 5\omega^2 a - 10a^3 + a^5/\omega^2$$

$$k_5 = -\omega^3 + 10\omega a^2 - 5\, a^4/\omega$$

with the Gaussian initial condition,

$$X_c \sim (\bar{X}_o \ , \ P_o) \quad , \tag{83}$$

and the white noise excitation process,

$$V \sim (O \ , \ S) \quad , \quad S = \begin{bmatrix} q & 0 \\ 0 & r \end{bmatrix} \tag{84}$$

The steady-state response to the white noise excitation process is a stochastic solution process which is characterized by the zero mean vector,

$$E\{X(t)\} = \bar{X} = 0 \quad , \tag{85}$$

and the constant covariance matrix

$$E\left\{X(t)X^T(t)\right\} = P = \text{const} \quad . \tag{86}$$

The covariance matrix P indicates the general information in the solution process. For the optimization, a criterion for the performance of the LST fine pointing system must be introduced. For this purpose, a scalar functional of the elements of the covariance matrix can be used. In particular, for the LST the standard deviation of the pitch motion

$$\sigma_\theta = \sigma_{x1} = \sqrt{P_{11}} \tag{87}$$

is an appropriate criterion directly characterizing the pointing stability. The covariance matrix P can be found by the spectral density analysis or by the covariance analysis of the stochastic differential equation (82). Both methods are outlined in the appendix. The covariance analysis is used here because it is better suited to systems of higher dimension.

The steady-state covariance matrix P can be computed from the algebraic matrix equation,

$$\bar{A}P + P\bar{A}^T + Q = 0 \quad , \tag{88}$$

where

$$Q = \bar{G}S\bar{G}^T \quad . \tag{89}$$

Equation (88) has a unique solution since the system (82) is asymptotically stable. Although the matrix equation (88) is linear in P , its solution cannot be directly found by simple matrix inversion. However, the expansion in linear equations is possible according to Chen and Shieh [12], and an explicit solution has been given by Müller [13]. Here, the method of Chen and Shieh is used for the numerical computation of P . Further, one element of P is obtained algebraically by the method of Müller. The symmetric matrices P and Q are written in Table 4.

The numerical computations are all done for the twice orbital rate $\omega = 2 \times 10^{-3}$ rad/sec, representing an altitude of 800 km, and for the sensor noise spectral density $r = 8.394 \times 10^{-6}$ arc sec^2 sec corresponding to a magnitude 12 guide star with a 20 arc min offset. The spectral density of the disturbance noise may be either $q = 0$ or $q = 1 \times 10^{-12}$ arc sec^2/sec^3 . The characteristic frequency is variable within the region $1 \times 10^{-3} < \alpha < 1 \times 10^{2}$ rad/sec. Some results obtained by the method of Chen and Shieh are given in Tables 5 and 6. The following phenomena can be interpreted: The solution process is almost completely correlated. Only P_{12} may be

TABLE 4. COVARIANCE MATRIX P AND
NOISE EXCITATION MATRIX Q

$$P = \begin{bmatrix} P_{11} & P_{12} & P_{13} & P_{14} & P_{15} & P_{16} & P_{17} \\ P_{12} & P_{22} & P_{23} & P_{24} & P_{25} & P_{26} & P_{27} \\ P_{13} & P_{23} & P_{33} & P_{34} & P_{35} & P_{36} & P_{37} \\ P_{14} & P_{24} & P_{34} & P_{44} & P_{45} & P_{46} & P_{47} \\ P_{15} & P_{25} & P_{35} & P_{45} & P_{55} & P_{56} & P_{57} \\ P_{16} & P_{26} & P_{36} & P_{46} & P_{56} & P_{66} & P_{67} \\ P_{17} & P_{27} & P_{37} & P_{47} & P_{57} & P_{67} & P_{77} \end{bmatrix} \qquad Q = \begin{bmatrix} 0 & 0 & 0 & 0 & 0 & 0 & 0 \\ 0 & q & 0 & 0 & 0 & 0 & 0 \\ 0 & 0 & k_1^2 r & k_1 k_2 r & k_1 k_3 r & k_1 k_4 r & k_1 k_5 r \\ 0 & 0 & k_1 k_2 r & k_2^2 r & k_2 k_3 r & k_2 k_4 r & k_2 k_5 r \\ 0 & 0 & k_1 k_3 r & k_2 k_3 r & k_3^2 r & k_3 k_4 r & k_3 k_5 r \\ 0 & 0 & k_1 k_4 r & k_2 k_4 r & k_3 k_4 r & k_4^2 r & k_4 k_5 r \\ 0 & 0 & k_1 k_5 r & k_2 k_5 r & k_3 k_5 r & k_4 k_5 r & k_5^2 r \end{bmatrix}$$

$k_1 = -5\alpha, \quad k_2 = \omega^2 - 10\alpha^2, \quad k_3 = \alpha^5/\omega^2$

$k_4 = 5\omega^2\alpha - 10\alpha^3 + \alpha^5/\omega^2, \quad k_5 = -\omega^3 + 10\omega\alpha^2 - 5\alpha^4/\omega$

generally vanishing, which means that the process of the pitch angle θ and the pitch velocity $\dot{\theta}$ are uncorrelated. The variance P_{11} or the standard deviation σ_θ is always less than the variance P_{13} or the standard deviation $\sigma_{\hat{\theta}}$ of the pitch estimation $\hat{\theta}$. This means that in addition to the dynamics of the observer or filter, the dynamics of the LST system itself are reducing the effect of the sensor noise to the pointing stability. Therefore, an optimal filter does not necessarily result in a minimal steady-state response of the pointing stability. Further, the following standard deviations σ_θ can be listed as functions of α and q (Table 7). The standard deviations σ_θ for $q = 0$ are always less than in the case of $q = 10^{-12}$ arc sec^2/sec^3 and appear to be monotonically decreasing with the characteristic frequency α, while for the case $q = 10^{-12}$ arc sec^2/sec^3 a minimum obviously exists.

To obtain more information on the variance P_{11} or the standard deviation σ_θ, respectively, this element of P will be evaluated algebraically.

The explicit solution for the covariance matrix P is, according to Müller [13]:

$$P = \frac{1}{2 \det H} \sum_{k=0}^{6} H_{k+1,1} \sum_{m=0}^{2k} (-1)^m A_m Q A_{2k-m}^T \qquad (90)$$

TABLE 5. COVARIANCE MATRICES FOR VARIOUS CHARACTERISTIC FREQUENCIES (q = 0)

$\alpha = 2\text{-}10^{-3}$ rad/sec			SOLUTION MATRIX P			q = 0
.255755-007	.000000	.211162-007	.477409-010	.115417-013	.839400-013	−.440685-013
	.370910-012	−.923340-010	.114892-013	−.356745-016	−.545610-016	.310578-015
		.756772-007	.125910-009	.451177-013	.186766-012	−.209850-012
			.530596-012	.100728-015	.507837-015	−.344154-015
				.293790-019	.125910-019	−.125910-018
					.671520-018	−.503640-018
						.671520-018
$\alpha = 2\text{-}10^{-2}$ rad/sec			SOLUTION MATRIX P			q = 0
.639533-006	.000000	.581504-006	.796502-008	.281528-002	−.257908-008	.132326-008
	.787404-009	−.137679-007	.319319-009	−.464230-010	.391574-010	−.279059-010
		.115585-005	.154641-007	.617288-008	−.555768-008	.305108-008
			.771641-009	.123713-009	−.113013-009	.577609-010
				.366191-010	−.330225-010	.179693-010
					.297919-010	−.161814-010
						.886027-011
$\alpha = 2\text{-}10^{-1}$ rad/sec			SOLUTION MATRIX P			q = 0
.645474-005	.423516-021	.587276-005	.800018-006	.283929-003	−.283691-003	.135063-004
	.792947-006	−.138201-005	.322124-006	−.465591-004	.464855-004	−.289487-005
		.116190-004	.154525-005	.619689-003	−.619069-003	.312081-004
			.774512-006	.123940-003	−.123833-003	.587480-005
				.367227-001	−.366865-001	.183579-002
					.366503-001	−.183396-002
						.922962-004

TABLE 6. COVARIANCE MATRICES FOR VARIOUS CHARACTERISTIC FREQUENCIES ($q = 1 \times 10^{-12}$ arc sec^2/sec^3)

α = 2-10^{-3} rad/sec			SOLUTION MATRIX P		q = 1-10^{-12} arc sec^2/sec^3	
.295924-003	.000000	.282248-003	−.113234-006	.101574-009	−.312416-009	−.203169-009
	.465215-009	−.235299-007	.183709-009	−.109411-012	−.313046-013	−.187189-012
		.270583-003	−.117062-006	.101608-009	−.296688-009	−.187710-009
			.152874-009	−.936493-013	.156758-012	−.628442-013
				.218779-015	−.623741-016	.623741-016
					.100067-014	.249496-015
						.100067-014

α = 2-10^{-2} rad/sec			SOLUTION MATRIX P		q = 1-10^{-12} arc sec^2/sec^3	
.774509-006	.000000	.712343-006	.797332-008	.331474-008	−.304778-008	.154694-008
	.870835-009	−.141899-007	.355466-009	−.497326-010	.416903-010	−.304650-010
		.128496-005	.152917-007	.667234-008	−.802355-008	.327994-008
			.791422-009	.122333-009	−.111947-009	.566720-010
				.388875-010	−.350979-010	.190986-010
					.317018-010	−.171983-010
						.945471-011

α = 2-10^{-1} rad/sec			SOLUTION MATRIX P		q = 1-10^{-12} arc sec^2/sec^3	
.645534-004	.277556-016	.587333-004	.800053-004	.283963+002	−.283951+002	.135091+000
	.793003-003	−.138206-003	.322152-003	−.465604+002	.465597+002	−.289592+000
		.116196-003	.154928-003	.619713+002	−.619707+002	.312151+000
			.774641-003	.123943+003	−.123942+003	.587579+000
				.367237+008	−.367234+008	.183618+006
					.367230+008	−.183616+006
						.923336+003

TABLE 7. STANDARD DEVIATIONS

σ_θ (arc sec)	q = 0	q = 10^{-12} arc sec^2/sec^3
$\alpha = 2 \times 10^{-3}$ rad/sec	1.599×10^{-4}	1.740×10^{-2}
$\alpha = 2 \times 10^{-2}$ rad/sec	7.997×10^{-4}	8.801×10^{-4}
$\alpha = 2 \times 10^{-1}$ rad/sec	2.540×10^{-3}	2.541×10^{-3}

where H is the Hurwitz matrix (71); $H_{k+1,1}$ is the cofactor of the element $h_{k+1,1}$ of H; $A_m = \bar{A}A_{m-1} + a_m E$ is a 7 × 7-matrix, and a_m is the corresponding coefficient of the characteristic equation (69). In particular, for P_{11} it yields

$$
\begin{aligned}
P_{11} = \frac{1}{2 \det H} \Big\{ & H_{11} Q_{11} + H_{21} [2(A_2 Q)_{11} - (A_1 Q A_1^T)_{11}] \\
& + H_{31} [2(A_4 Q)_{11} - 2(A_1 Q A_3^T)_{11} + (A_2 Q A_2^T)_{11}] \\
& + H_{41} [2(A_6 Q)_{11} - 2(A_1 Q A_5^T)_{11} + 2(A_2 Q A_4^T)_{11} - (A_3 Q A_3^T)_{11}] \\
& + H_{51} [2(A_2 Q A_6^T)_{11} - 2(A_3 Q A_5^T)_{11} + (A_4 Q A_4^T)_{11}] \\
& + H_{61} [2(A_4 Q A_6^T)_{11} - (A_5 Q A_5^T)_{11}] \\
& + H_{71} (A_6 Q A_6^T)_{11} \Big\}
\end{aligned}
\tag{91}
$$

All cofactors, matrix elements, and the Hurwitz determinant are listed in Table 8 as a function of α, ω, q, and r. From Table 8, one immediately obtains with equation (91) the following result:

TABLE 8. DETERMINANT, COFACTORS AND MATRIX ELEMENTS FOR CALCULATION OF VARIANCE P_{11}

DETERMINANT	$\det H = 2\,097\,152a^{28}$
COFACTORS	$H_{11} = 437\,088a^{27}$ $H_{12} = -43\,008a^{25}$ $H_{13} = 14\,336a^{23}$ $H_{14} = -10\,240a^{21}$ $H_{15} = 14\,336a^{19}$ $H_{16} = -43\,008a^{17}$ $H_{17} = 437\,088a^{15}$
MATRIX ELEMENTS	$Q_{11} = (A_2Q)_{11} = (A_4Q)_{11} = (A_6Q)_{11} = 0$ $(A_1QA_1^T)_{11} = q$ $(A_1QA_3^T)_{11} = 21a^2q$ $(A_1QA_5^T)_{11} = -\omega^4q + 21\omega^2a^2q$ $(A_2QA_2^T)_{11} = 49a^2q + 49\omega^4a^2r - 490\omega^2a^4r + 1225a^6r$ $(A_2QA_4^T)_{11} = 49\omega^2a^2q - 147\omega^2a^6r + 735a^8r$ $(A_2QA_6^T)_{11} = -7\omega^2a^8r + 35a^{10}r$ $(A_3QA_3^T)_{11} = 441a^4q + \omega^8r - 42\omega^6a^2 + 511\omega^4a^2r$ $-1470\omega^2a^6r + 1225a^8r$ $(A_3QA_5^T)_{11} = -21\omega^4a^2q + 441\omega^2a^4q + 7\omega^4a^6r$ $-147\omega^2a^8r + 245a^{10}r$ $(A_4QA_4^T)_{11} = 49\omega^4a^2q + 441a^{10}r$ $(A_4QA_6^T)_{11} = 21a^{12}r$ $(A_5QA_5^T)_{11} = \omega^8q - 42\omega^6a^2q + 441\omega^4a^4q + 49a^{12}r$ $(A_6QA_6^T)_{11} = a^{14}r$

$$P_{11} = \frac{1}{2048}(2275\,\alpha^{-3} - 6454\,\omega^2\alpha^{-5} + 9888\,\omega^4\alpha^{-7} - 882\,\omega^6\alpha^{-9}$$

$$+ 21\,\omega^8\alpha^{-11})q + \frac{1}{2048}(7875\,\alpha - 7350\,\omega^2\alpha^{-1} + 2800\,\omega^4\alpha^{-3}$$

$$- 210\,\omega^6\alpha^{-5} + 5\omega^8\alpha^{-7})r \quad . \tag{92}$$

Thus, it results that the variance P_{11} is a linear combination of the disturbance noise term characterized by q and the sensor noise term given by r. For low characteristic frequencies, one obtains

$$P_{11} \approx \frac{21}{2048}\,\omega^8\alpha^{-11}\,q + \frac{5}{2048}\,\omega^8\alpha^{-7}r \quad \text{for } \alpha \ll \omega \quad , \tag{93}$$

whereas for high characteristic frequencies it yields

$$P_{11} \approx \frac{7875}{2048}\,\alpha r \quad \text{for } \alpha \gg \omega \quad . \tag{94}$$

The limit cases, $\alpha \to 0$ and $\alpha \to \infty$, result both in $P \to \infty$ even if the disturbance noise vanishes, i.e., $q = 0$. Thus, there will be at least one minimum, depending generally on the ratio q/r. But the most interesting case is $q = 0$, for which Table 7 indicated a monotonically decreasing function of the characteristic frequency α. The extrema of P_{11} can be found from

$$dP_{11}/d\alpha = 0 \quad . \tag{95}$$

Using equation (92) with $q = 0$, it follows from equation (95) that

$$225 + 210\,\omega^2\alpha^{-2} - 240\,\omega^4\alpha^{-4} + 30\,\omega^6\alpha^{-6} - \omega^8\alpha^{-8} = 0 \quad . \tag{96}$$

According to Descartes' rule, equation (96) has one or three positive roots for the variable $\omega\alpha^{-1}$. It turns out that three positive roots exist, which are listed in Table 9.

TABLE 9. EXTREMA OF STANDARD DEVIATION

Root No.	α/ω	σ_θ (arc sec)
1	0.258199	3.903×10^{-4}
2	0.268824	3.905×10^{-4}
3	0.750895	1.247×10^{-4}

The roots Nos. 1 and 3 represent the minima, and No. 3 is the absolute minima. In Figure 8, the standard deviation σ_θ or pointing stability is shown as a function of the characteristic frequency. The absolute minimum found for q = 0 occurs at $\alpha = 1.5 \times 10^{-3}$ rad/sec and for $q = 10^{-12}$ arc sec^2/sec^3 at $\alpha = 1.8 \times 10^{-2}$ rad/sec. With these optimizations, the controller is completely defined. The characteristic frequency of the pointing system is, in each case, far below the bending frequencies.

Finally, some comments on the disturbance accommodation controller may be useful. The original approach of the disturbance accommodation presented by Johnson [7, 8] is very well suited for a completely deterministic system given by equations (41) and (42). However, if there is some sensor noise within the system, the advantage of the disturbance accommodation may completely fade away because of the system's response to the sensor noise. Therefore, the disturbance accommodation controller must be optimized with respect to the standard deviation of the steady-state noise response. Such controllers will be called Disturbance Accommodation Standard deviation Optimal Controllers (DASOC). The recommendation of Johnson to use fast settling times for the observer-accommodator will result in large negative eigenvalues representing high frequencies in the closed-loop system. However, high frequencies amplify the sensor noise heavily. On the other hand, the well-known technique using low frequencies for the reduction of the system's sensor noise response will not work either. Even if all disturbances are exactly cancelled out, the sensor noise may be strongly amplified within the accommodator loop of the controller. Somewhere between low and high frequencies, there will be an optimum. As pointed out in the section, Stability and Transient Response, at least one free parameter of the closed-loop system must be available for the variation of the system's frequencies or eigenvalues to obtain an optimum.

SENSITIVITY ANALYSIS OF THE DASOC SYSTEM

In the previous section, the DASOC was completely defined, and the steady-state response to constant and sinusoidal disturbance torques was designed to be zero if the disturbance frequency is exactly known. However, the disturbance frequency or twice orbital rate is slowly time-varying and the question arises as to the sensitivity of the DASOC to frequency deviations. The sensitivity can be determined by means of the closed-loop system's steady-state response to the deterministic disturbances.

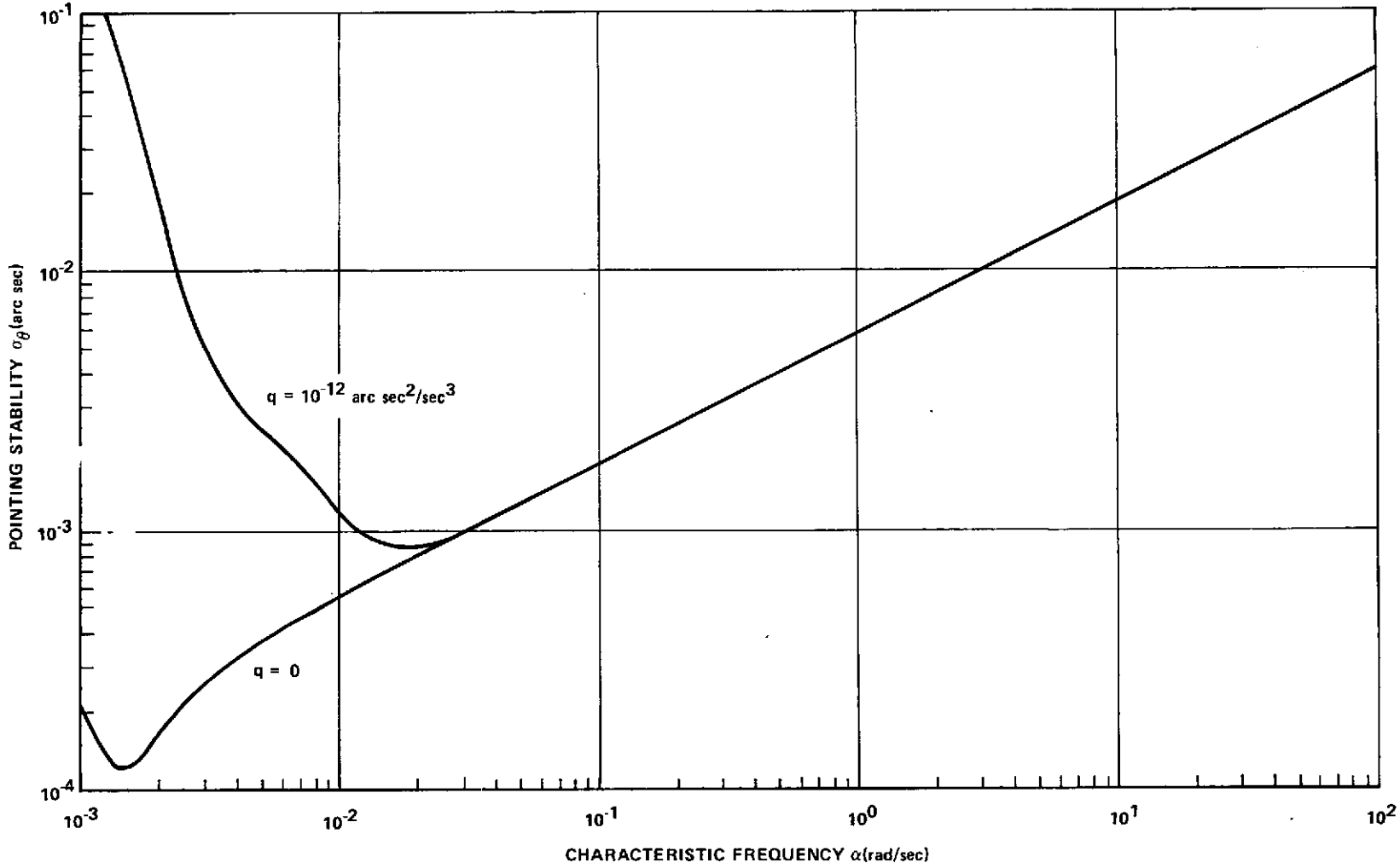

Figure 8. Pointing stability for various disturbances.

The response to the constant and sinusoidal disturbances depends on the deterministic part of differential equation (60) written as

$$\dot{X} = \bar{A}X + \bar{F}W \tag{97}$$

with the scalar excitation

$$W = \beta + \gamma \cos(\Omega t + \chi) \quad , \tag{98}$$

where Ω is an arbitrary frequency. Since equation (97) is linear, the constant and the sinusoidal disturbances can be treated separately.

The steady-state response of the asymptotically stable system (97) to a constant disturbance

$$W_\beta = \beta \tag{99}$$

is also a constant response

$$X_\beta = \text{const} \quad , \quad \dot{X}_\beta \equiv 0 \quad . \tag{100}$$

The substitution of equations (99) and (100) in the system equation (97) results in

$$\bar{A}X_\beta + \bar{F}\beta = 0 \quad , \tag{101}$$

with the solution,

$$X_\beta = \bar{A}^{-1}\bar{F}\beta = [0 \;\; 0 \;\; 0 \;\; 0 \;\; \beta \;\; 0 \;\; 0]^T \quad . \tag{102}$$

The solution (102) has been obtained using the matrices of Table 3. The steady-state response of the pitch motion is exactly zero, $\theta_\beta \equiv 0$, independent of the twice orbital

rate ω . The estimation of the constant disturbance in the steady state is exactly correct, i.e., $\hat{z}_1 = \beta$.

For the computation of the frequency response of the system (97), it is useful to introduce complex functions. The sinusoidal disturbances will be represented by

$$W_\gamma = \gamma \cos(\Omega t - \chi) = \gamma_c \cos \Omega t + \gamma_s \sin \Omega t$$

$$= f e^{i\Omega t} + \bar{f} e^{-i\Omega t} \tag{103}$$

where

$$f = \frac{1}{2}(\gamma_c - i\gamma_s) = \frac{1}{2}(\gamma \cos \chi - i\gamma \sin \chi) \quad . \tag{104}$$

The steady-state response is also a sinusoidal vector function:

$$X_\gamma = g e^{i\Omega t} + \bar{g} e^{-i\Omega t} \tag{105}$$

where

$$X_{\gamma i} = \xi_i \cos(\Omega t + \chi_i) = \xi_{ci} \cos \Omega t + \xi_{si} \sin \Omega t \tag{106}$$

and

$$g_i = \frac{1}{2}(\xi_{ci} - i\xi_{si}) \quad , \qquad i = 1(1)7 \quad . \tag{107}$$

With equations (103) and (105), it follows from the system equation (97) that

$$g = (i\Omega E - \bar{A})^{-1} \bar{F} \cdot f = Rf \quad . \tag{108}$$

The complex vector

$$R = \frac{\text{adj}\,(i\Omega E - \bar{A}) \cdot \bar{F}}{\det\,(i\Omega E - \bar{A})} \tag{109}$$

has elements of the form

$$R_i = \frac{x_i + iy_i}{u_o + iv_o} \quad . \tag{110}$$

Therefore, the amplitudes ξ_i of the solution vector elements (106) are

$$\xi_i = \sqrt{\frac{x_i^2 + y_i^2}{u_o^2 + v_o^2}}\ \gamma \quad . \tag{111}$$

Thus, the problem is reduced to the calculation of the vector R by means of the matrices in Table 3. The result is presented in Table 10. For arbitrary disturbance frequencies Ω , the response is not vanishing. However, disturbances with the design frequency $\omega = \Omega$ are cancelled out:

$$X_\gamma\,(\Omega = \omega) = [0 \quad 0 \quad 0 \quad 0 \quad 0 \quad \gamma \cos(\omega t - \chi)\,, \; -\gamma \sin(\omega t - \chi)]^T \quad . \tag{112}$$

Notice that the observer-accommodator creates a correct estimation of the sinusoidal disturbance $\hat{z}_2 = \gamma \cos(\omega t - \chi)$, not only in amplitude but also in phase angle.

The pointing stability of the LST is a function of the pitch motion. Therefore, the pitch motion amplitude, $\xi_\theta = \xi_1$ will be evaluated in more detail now. One obtains from Table 10,

$$x_1 = 7\alpha\Omega^4 - 7\omega^2\alpha\Omega^2 \quad , \tag{113}$$

$$y_1 = \Omega^5 - 21\alpha^2\Omega^3 - (\omega^4 - 21\omega^2\alpha^2)\Omega \quad , \tag{114}$$

TABLE 10. COMPLEX FREQUENCY RESPONSE COMPONENTS

COMPONENT NO.	COMPLEX COMPONENT
1	$\frac{i\Omega(-\Omega^2+\omega^2)}{\det(i\Omega E-\bar{A})}\left[(-\Omega^2-\omega^2+21a^2)+i7a\Omega\right]$
2	$\frac{-\Omega^2(-\Omega^2+\omega^2)}{\det(i\Omega E-\bar{A})}\left[(-\Omega^2-\omega^2+21a^2)+i7a\dot{\Omega}\right]$
3	$\frac{i\Omega(-\Omega^2+\omega^2)}{\det(i\Omega E-\bar{A})}\left[(20a^2-\omega^2)+i5a\Omega\right]$
4	$\frac{i\Omega(-\Omega^2+\omega^2)}{\det(i\Omega E-\bar{A})}\left[-5a^2+i(\omega^2-10a^2)\Omega\right]$
5	$\frac{-(-\Omega^2+\omega^2)}{\det(i\Omega E-\bar{A})}\left[(-\Omega^2+a^2)+i2a\Omega\right]$
6	$\frac{\Omega^2 k_4-i\Omega\omega k_5}{\det(i\Omega E-\bar{A})}\left[(-\Omega^2+a^2+i2a\Omega)\right]$
7	$\frac{\Omega^2 k_5+i\Omega\omega k_4}{\det(i\Omega E-\bar{A})}\left[(-\Omega^2+a^2+i2a\Omega)\right]$

$$k_4 = 5\omega^2 a - 10a^3 + a^5/\omega^2 \quad , \quad k_5 = -\omega^3 + 10\omega a^2 - 5a^4/\omega \, ,$$

$$\det(i\Omega E - \bar{A}) = \left[-7a\Omega^6 + 35a^3\Omega^4 - 21a^5\Omega^2 + a^7\right] + i\left[-\Omega^7 + 21a^2\Omega^5 - 35a^4\Omega^3 + 7a^6\Omega\right]$$

$$u_0 = -7\alpha\Omega^6 + 35\alpha^3\Omega^4 - 21\alpha^5\Omega^2 + \alpha^7 \quad , \tag{115}$$

and

$$v_0 = -\Omega^7 + 21\alpha^2\Omega^5 - 35\alpha^4\Omega^3 + 7\alpha^6\Omega \quad . \tag{116}$$

Introducing the equations (113) through (116) in equation (111), the amplitude ratio ξ_θ/γ of the pitch motion frequency response can be easily computed. In Figures 9 through 11, the ratio ξ_θ/γ is shown as a function of the actual disturbance frequency Ω for various characteristic frequencies α. The disturbance accommodation point $\Omega = \omega$ is obvious. Further, one realizes that the sensitivity to frequency deviations is rapidly increasing with decreasing characteristic frequencies. For small frequency deviations

$$\Omega = \omega(1 + \epsilon) \quad , \qquad \epsilon \ll 1 \quad , \tag{117}$$

the amplitude ξ_θ is directly proportional to the error ϵ, having the form

$$\xi_\theta = \frac{1}{\omega^2}\sqrt{\frac{\kappa_1^2 + \kappa_2^2}{\kappa_3^2 + \kappa_4^2}}\ \gamma\epsilon \tag{118}$$

where

$$\kappa_1 = 14\alpha\omega^{-1} \quad , \quad \kappa_2 = 4 - 42\alpha^2\omega^{-2} \quad .$$

$$\kappa_3 = -7\alpha\omega^{-1} + 35\alpha^3\omega^{-3} - 21\alpha^5\omega^{-5} + \alpha^7\omega^{-7} \quad ,$$

$$\kappa_4 = -1 + 21\alpha^2\omega^{-2} - 35\alpha^4\omega^{-4} + 7\alpha^6\omega^{-6} \quad . \tag{119}$$

To get an idea of the real magnitude of the amplitude ξ_θ affecting the pointing stability, let us assume the worst gravity-gradient torque and a vanishing magnetic torque. For $I_x \ll I_y = I_z$, $g_{y2} = 1$ and $m_0 = 0$, it follows from equation (30) that

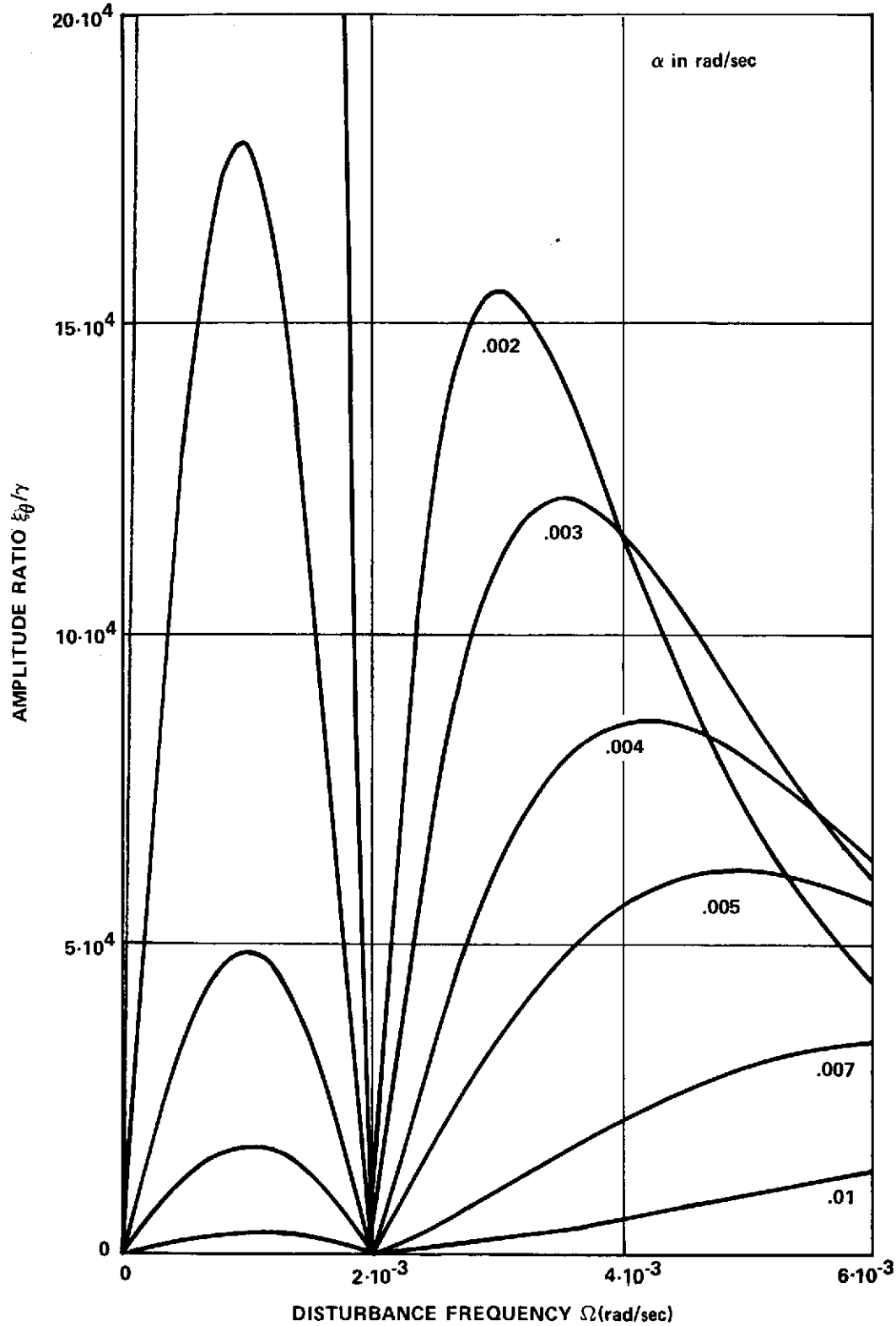

Figure 9. Frequency response for various characteristic frequencies ($2 \times 10^{-3} \leqslant \alpha \leqslant 10^{-2}$).

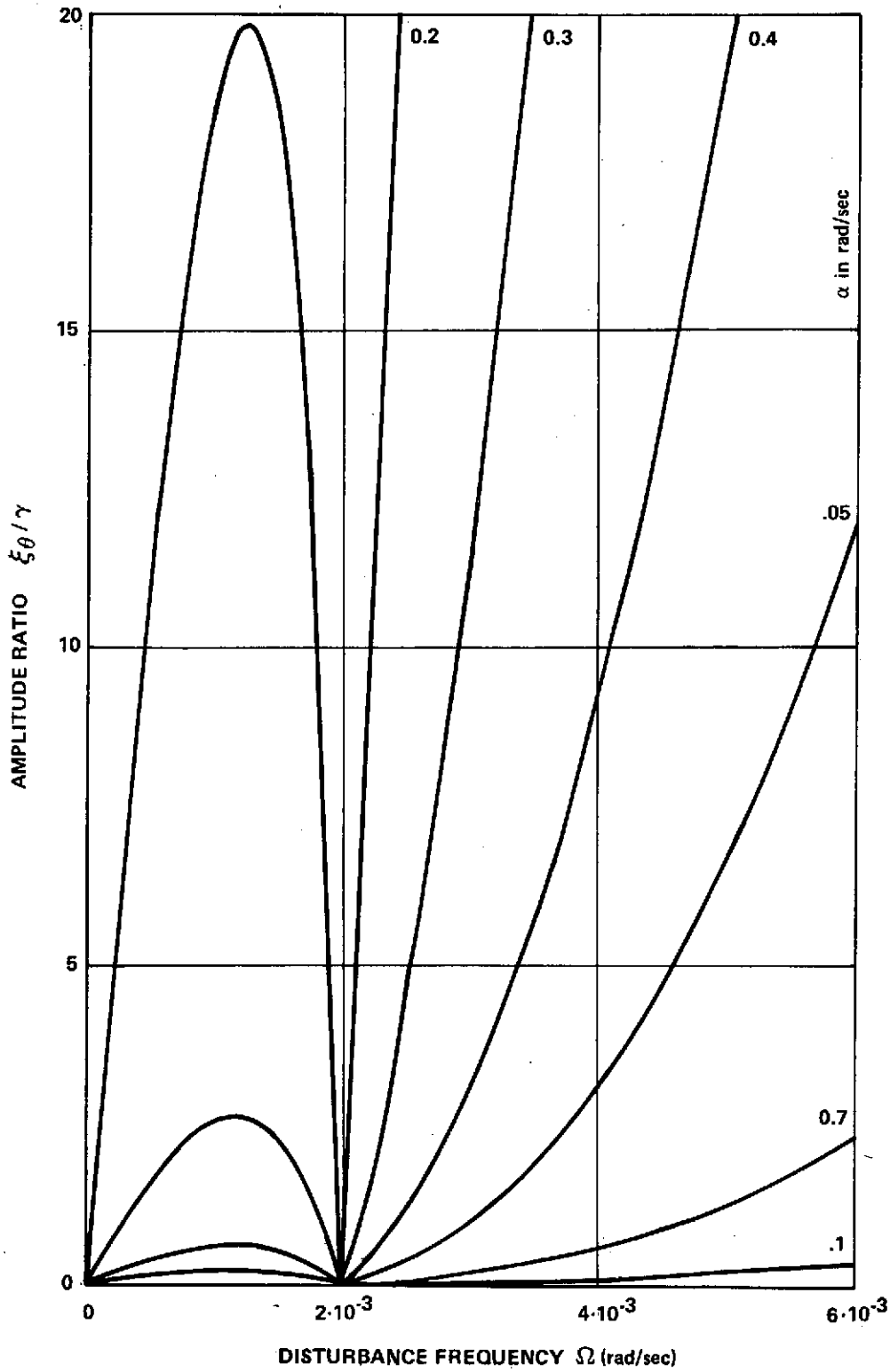

Figure 10. Frequency response for various characteristic frequencies ($2 \times 10^{-2} \leqslant \alpha \leqslant 10^{-1}$).

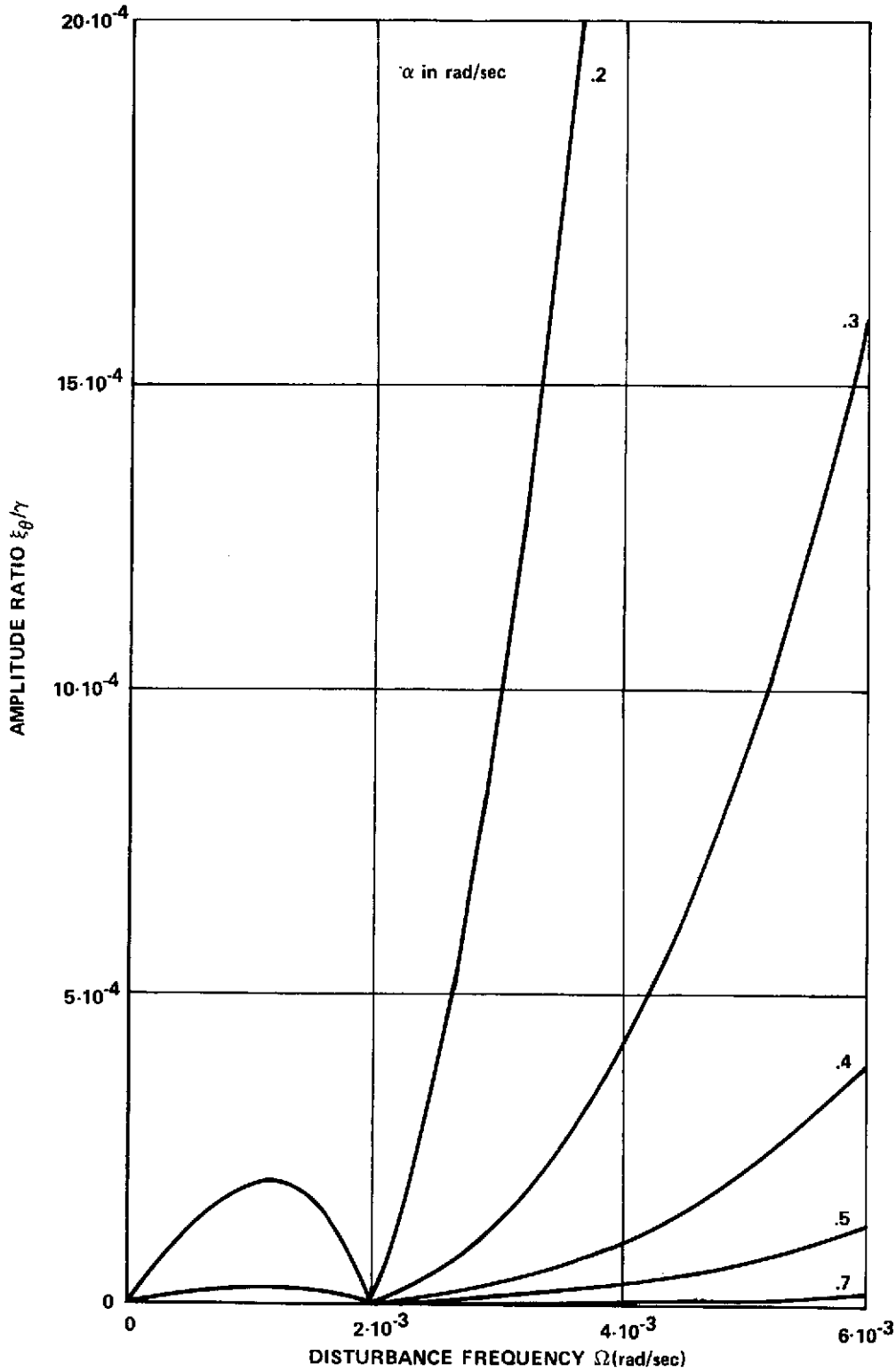

Figure 11. Frequency response for various characteristic frequencies ($2 \times 10^{-1} \leqslant \alpha \leqslant 1$).

$$\gamma = \frac{3}{8}\,\omega^2 \quad . \tag{120}$$

Introducing equation (120) in equation (118) and using the identity 1 rad = 206 264 arc sec, a sensitivity factor is defined as

$$\xi_\theta/\epsilon = 77349\,\sqrt{\frac{\kappa_1^2 + \kappa_2^2}{\kappa_3^2 + \kappa_4^2}} \tag{121}$$

where ξ_θ is given in arc seconds. In particular, for $\alpha \gg \omega$, equation (122) becomes

$$\xi_\theta/\epsilon = 3\,248\,658\,\omega^5\,\alpha^{-5} \quad . \tag{122}$$

The sensitivity factor ξ_θ/ϵ is plotted in Figure 12 as a function of the characteristic frequency. It is obvious again that the sensitivity is strongly decreasing with the increasing characteristic frequency α.

The frequency response characterized by ξ_θ can be added to the noise response σ_θ to obtain the resulting root mean square error or pointing stability:

$$\mathrm{rms}_\theta = \sqrt{\sigma_\theta^2 + \xi_\theta^2} \quad . \tag{123}$$

In Figure 13, the pointing stability (123) is shown for various errors of the disturbance frequency and vanishing noise disturbance, q = 0. The optimal performances are listed in Table 11.

Thus the twice orbital rate ω must be adjusted accurately within the DASOC to obtain full advantage. This can be realized by updating during the mission. But even if the orbital rate is not adjusted, resulting in $\epsilon = 10^{-1}$, the DASOC will still meet the requirement on the LST pointing stability with some margin.

COMPARISON WITH CONVENTIONAL SYSTEMS

Thus far the DASOC has shown good behavior, but unquestionably this sophisticated controller results in more complex hardware and increasing costs. By

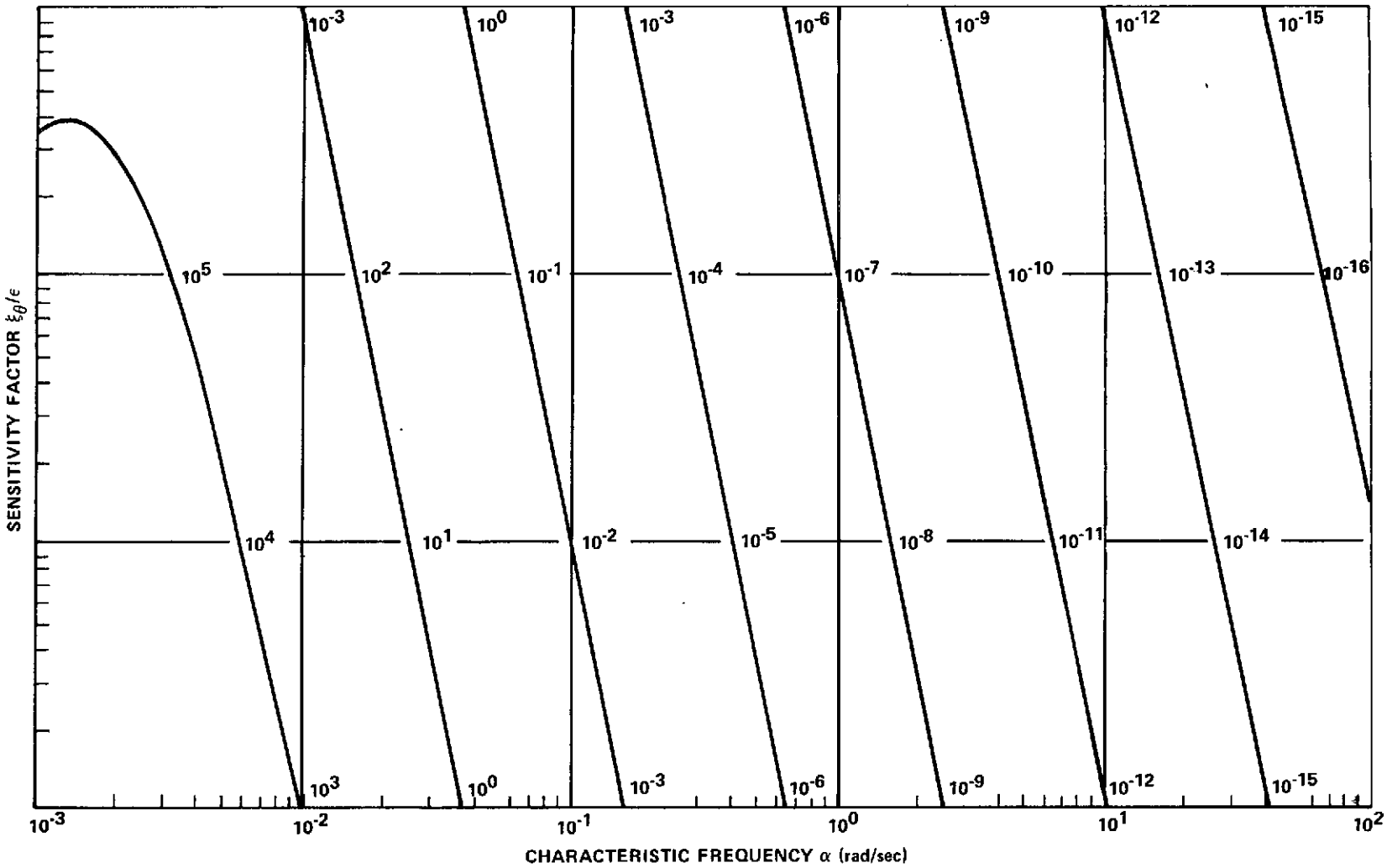

Figure 12. Sensitivity factor.

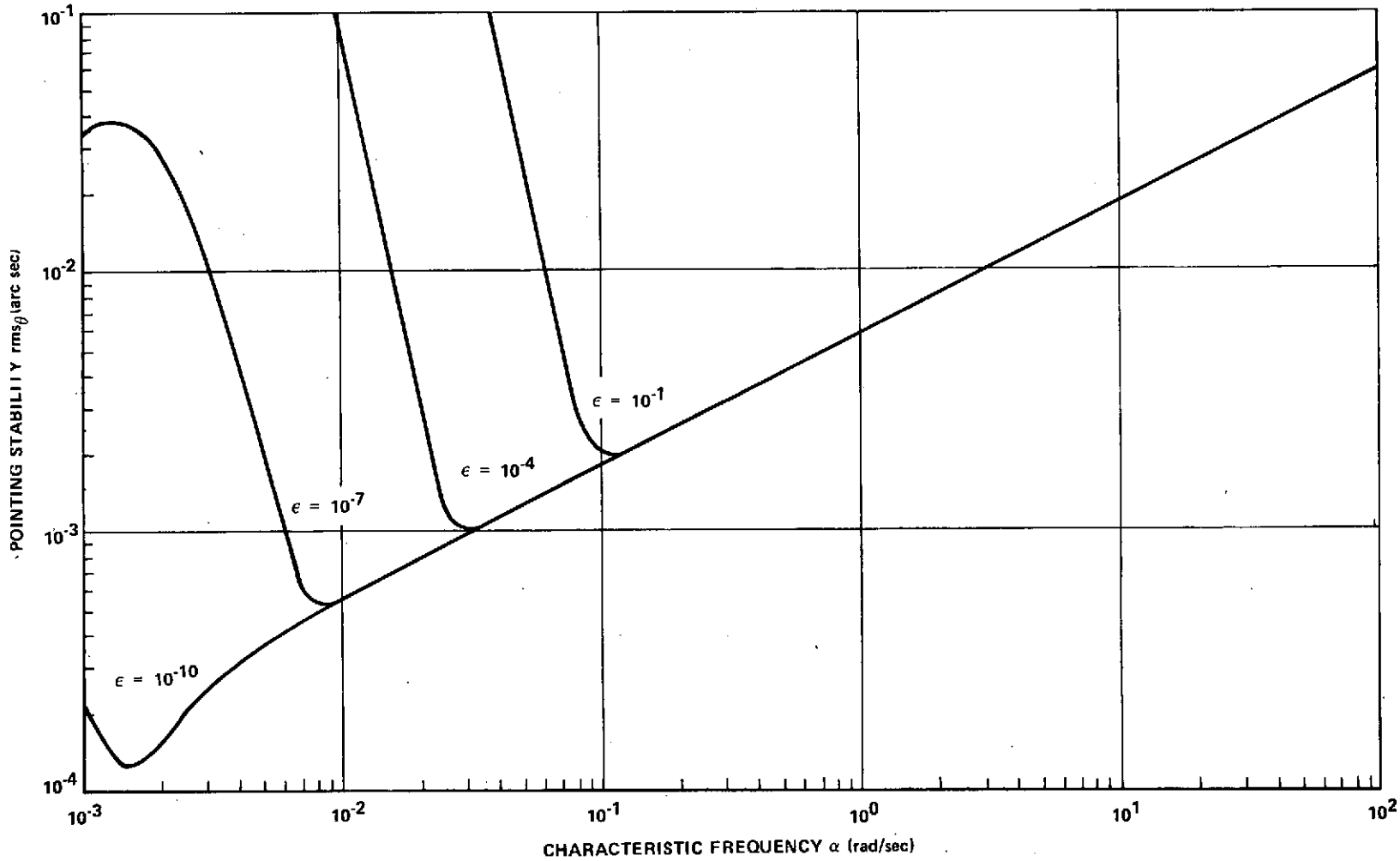

Figure 13. Pointing stability for various frequency errors.

TABLE 11. OPTIMA OF POINTING STABILITY

ϵ	rms_θ min (arc sec)
10^{-10}	1.27×10^{-4}
10^{-7}	5.45×10^{-4}
10^{-4}	1.05×10^{-3}
10^{-1}	1.99×10^{-3}

comparison with the simple conventional controllers, it can be determined if the DASOC is worth the additional expense. The conventional controllers PC, PIC, and PI^2C designed by Proise [4] will be used in the comparison. Control systems with different kinds of controllers are comparable if identical inputs are used and the same outputs are observed. This means that according to Reference 5, aerodynamic and solar pressure torques are not included, $q = 0$, and a correct orbital rate adjustment within the DASOC is assumed, $\epsilon = 0$. The standard deviation σ_θ is equivalent to the rms_θ obtained in Reference 5. Both quantities describe the pointing stability as a function of a corresponding characteristic frequency α.

The comparison is shown in Figure 14, together with the structural bending frequencies given in the reference cited in the footnote, p. 1. As mentioned earlier, the PI^2C results in a factor of 3 improvement in pointing stability and a factor of 9 reduction of the optimal characteristic frequency with respect to the PC. Compared with the PI^2C, the DASOC offers a factor of 30 improvement in pointing stability and a factor of 500 reduction of optimal characteristic frequency.

The actual requirement on the LST pointing accuracy is stabilization within 0.005 arc sec rms. Figure 14 indicates that the PC does not meet this requirement. The PIC meets the 0.005 arc sec with little margin, and the PI^2C is scarcely better. On the other hand, the DASOC easily meets the requirement, and a large safety factor remains for the compensation of possible deteriorations. Some additional errors may be caused by aerodynamic and solar pressure torques and incorrect orbital rate adjustments. Also, the extreme accuracy of the DASOC allows greater tolerance on other sources of errors such as the Control Moment Gyro (CMG) and reaction wheel vibrations, bending modes, nonlinearities, etc.

The characteristic frequency α is generally not identical with the frequencies in the transient response. These depend on the eigenvalues of the closed-loop pointing system. Therefore, it is useful to compare the eigenvalue distribution of different controllers. The eigenvalues can be found from the characteristic equation. According to Reference 5, the characteristic equation of the closed-loop system with the PC reads as

$$\lambda^3 + 5.62\alpha\lambda^2 + 10\alpha^2\lambda + 5.62\alpha^3 = 0 \quad . \tag{124}$$

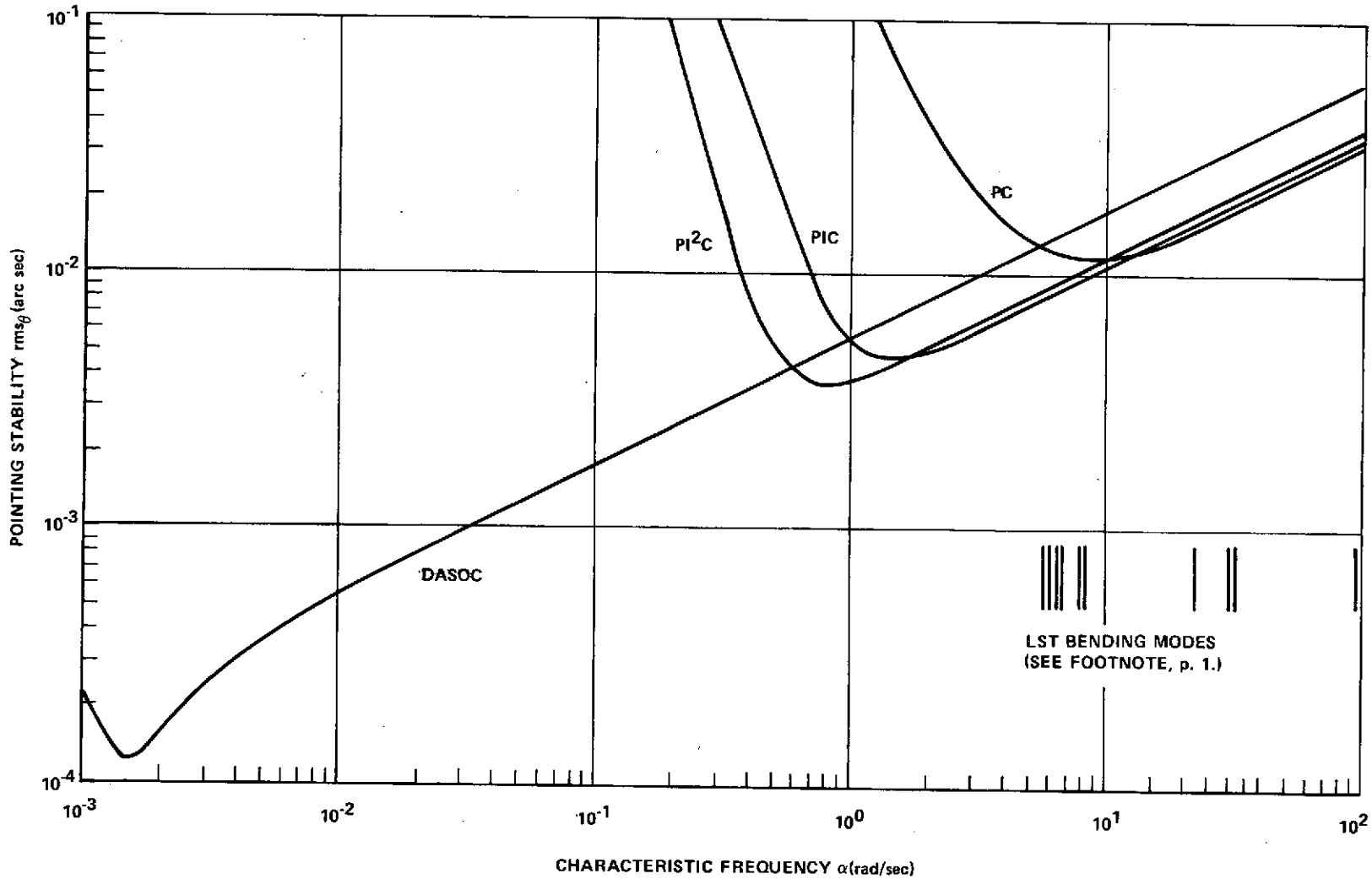

Figure 14. Pointing stability for different controllers.

The corresponding eigenvalues are

$$\lambda_1 = -1.18\,\alpha \quad , \quad \lambda_2 = -1.81\,\alpha \quad , \quad \lambda_3 = -2.63\,\alpha \quad . \tag{125}$$

With the PIC, one obtains

$$\lambda^4 + 5.62\,\alpha\lambda^3 + 10\,\alpha^2\lambda^2 + 6.75\,\alpha^3\lambda + 0.635\,\alpha^4 = 0 \quad , \tag{126}$$

and the eigenvalues

$$\lambda_1 = -0.111\,\alpha \quad , \quad \lambda_2 = -3.03\,\alpha \quad , \quad \lambda_{3,4} = -1.25\,\alpha \pm 0.57\,\alpha i \quad . \tag{127}$$

With the PI^2C, it follows that

$$\lambda^5 + 5.62\,\alpha\lambda^4 + 10\alpha^2\lambda^3 + 6.75\,\alpha^3\lambda^2 + 0.663\,\alpha^4\lambda + 0.0178\,\alpha^5 = 0 \tag{128}$$

and the eigenvalues

$$\lambda_{1,2} = -0.056\,\alpha \quad , \quad \lambda_3 = -3.03\,\alpha \quad , \quad \lambda_{4,5} = -1.25\,\alpha \pm 0.57\,\alpha i \quad . \tag{129}$$

The characteristic equation of the system with the DASOC has been developed in the section, Stability and Transient Response. The characteristic equation (74) is simply

$$(\lambda + \alpha)^7 = 0 \tag{130}$$

and the sevenfold eigenvalue is

$$\lambda_i = -\alpha \quad , \quad i = 1(1)7 \quad . \tag{131}$$

All eigenvalues are presented in Figure 15.

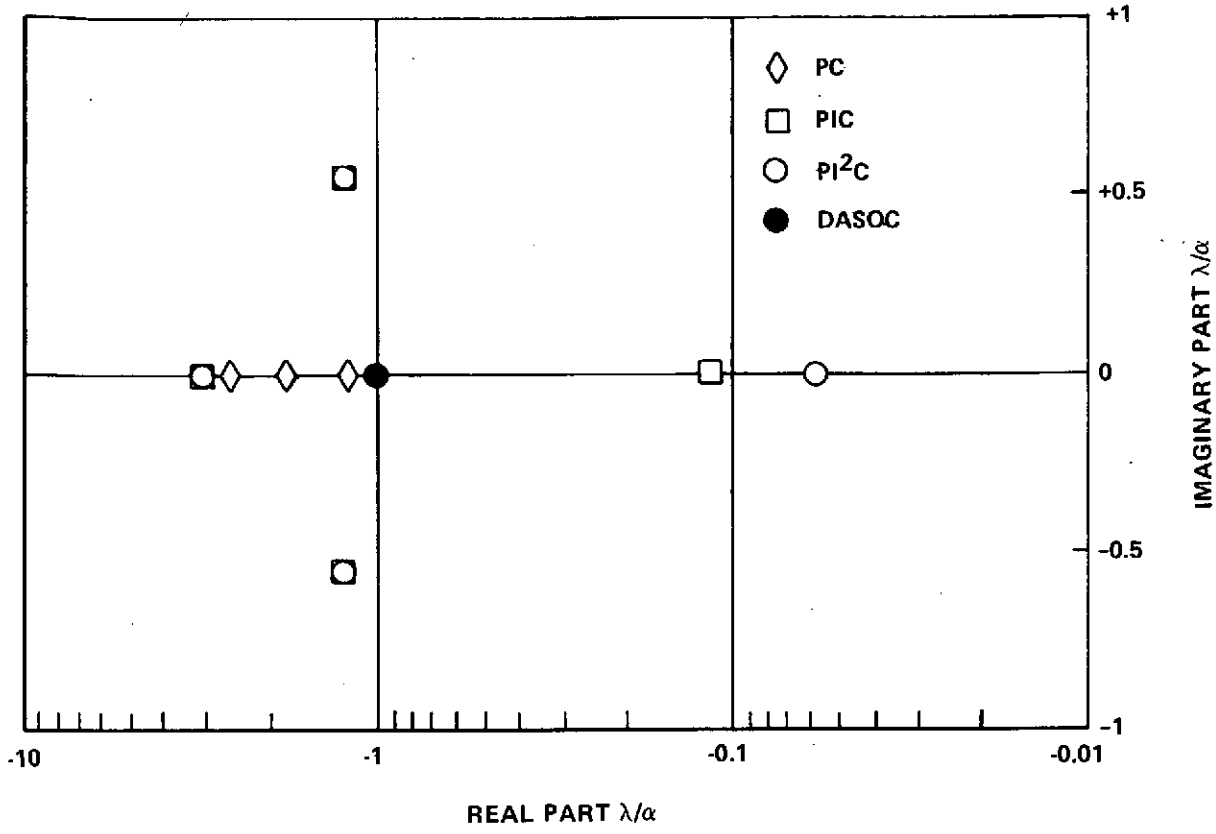

Figure 15. Eigenvalues for different controllers.

It is clear that especially for the system with the PI^2C, the eigenvalues are widely spread. For the characteristic frequency α the eigenvalues for the PI^2C are contained in the region, $0.052\alpha < \lambda < 3\alpha$. The eigenvalue, $\lambda = 0.05\alpha$, results in an unnecessarily large settling time, whereas the eigenvalue $\lambda = 3\alpha$ enhances the interaction with the structural bending modes. From these points of view, the DASOC has the optimal eigenvalue distribution.

The optimal characteristic frequency of the fine pointing system with the DASOC has been found as $\alpha = 1.5 \times 10^{-3}$ rad/sec in the limit case $q = 0$, $\epsilon = 0$. This means a large settling time of the order of magnitude of the orbit period. Such a large settling time may be acceptable during fine pointing operations, but it is not acceptable for LST maneuvering. However, this should not present a problem because maneuvering will be accomplished by CMG's and not the reaction wheels.

CONCLUSIONS

The LST fine body pointing to within 0.005 arc sec rms is the subject of this report. This difficult requirement on pointing stability is necessary to take full advantage of all the benefits from the diffraction-limited telescope.

The LST is modeled as a rigid body with three orthogonally mounted reaction wheel actuators. Nonlinear coupling phenomena do not appear, and, therefore, only a single axis analysis is performed. The principal disturbance torques result from the gravity-gradient and the magnetic desaturation system. Both are characterized by a constant term and a sinusoidal function of time with twice orbital rate. The fine guidance sensor providing the measurement of the spacecraft attitude motion generates a signal cluttered with electronic noise. Altogether, the LST is represented by a linear time-invariant system with deterministic and stochastic disturbances.

From earlier studies, it is known that the pointing stability of the LST with conventional controllers is limited by the external torques as well as by the sensor noise. Therefore, a more sophisticated controller is designed, using the recently developed technique of the accommodation of external disturbances to avoid the stability limitation caused by the external torques. Such a controller is constructed of three different loops: (1) an observer for the reconstruction of the complete state, (2) a regulator for the state feedback, and (3) an accommodator for the cancellation of the disturbance torques. The existence of a disturbance accommodation controller for the LST is proven by controllability and observability analyses. However, seven parameters or control gains remain to be determined. The stability analysis yields constraints on these free parameters, and within these constraints the parameters are optimized with respect to the transient response and the steady-state noise response. The transient response is found to be optimal for a sevenfold, real, negative eigenvalue. The magnitude of the multiple eigenvalue, the characteristic frequency, is then used for the steady-state noise response optimization. The steady-state response to the noise inputs is characterized by the covariance matrix and has been computed by the covariance equation widely used in estimation theory. In particular, for the standard deviation of the pointing motion, an algebraic formula was obtained. Then the optimal standard deviation was easily found. The result is the DASOC. In contrast to the original disturbance accommodation technique, the DASOC takes care not only of the external disturbances but also of the internal sensor noise.

Thus far the LST spacecraft with the DASOC has the following properties:

1. The asymptotic stability of the system is a priori guaranteed.

2. The system has only one characteristic frequency (multiple root) far below the bending frequencies of the LST structure.

3. The constant and the sinusoidal disturbance torques with twice orbital rate are completely cancelled out.

4. The steady-state standard deviation of the attitude motion or pointing stability is a function of the characteristic frequency.

5. An optimal pointing stability is maintained.

The frequency response to an external disturbance with variable frequency is used to define the sensitivity of the DASOC to the orbital rate adjustment. It turns out that updating of the orbital rate simulated in the DASOC is necessary to obtain good results.

In a comparison with the best conventional controller found in earlier studies, the DASOC offers up to a factor of 30 improvement in pointing stability, resulting in an optimal performance of nearly 0.0001 arc sec rms. In addition, the optimal characteristic frequency is reduced by a factor of 500. This means the DASOC easily meets the LST pointing stability requirement of 0.005 arc sec rms, even if aerodynamic and solar pressure torques as well as incorrect orbital rate adjustments are admitted. Excitation of vibrations in the LST structure by the DASOC is not expected to be a problem.

Further effort is necessary to apply the DASOC to more realistic spacecraft models and actuator systems and to perform a three-axis simulation. But the large-scale improvement with the DASOC allows a significant margin before the requirements of the LST are exceeded.

George C. Marshall Space Flight Center
National Aeronautics and Space Administration
Marshall Space Flight Center, Alabama, 35812, April 4, 1973

APPENDIX

RESPONSE OF LINEAR DIFFERENTIAL EQUATIONS TO WHITE NOISE

Stochastic differential equations are widely used in control theory. In the 1940's, the analysis of linear differential equations driven by white noise was conducted primarily in the frequency domain, using the spectral density. Since the 1960's, stochastic differential equations have been investigated in the time domain especially in connection with the development of the Kalman-Bucy filter using covariance matrices. Both methods, the spectral density analysis and the covariance analysis, will be reviewed briefly with respect to the application for the LST. Reference is made to James, Nichols, and Phillips [14] and to Bucy and Joseph [15].

The linear differential equation system

$$\dot{x} = Ax + Bw \quad , \quad x(t_0) = x_0 \sim (m_0 \, , P_0) \quad , \tag{A-1}$$

may be given by the $n \times 1$-state vector $x(t)$, the $r \times 1$-excitation vector $w(t)$, the $n \times n$-matrix A, and the $n \times r$-matrix B. Both matrices will be time invariant, and the matrix A will have eigenvalues with negative real parts only; i.e., the system (A-1) will be asymptotically stable. The initial condition $x(t_0)$ is given by a Gaussian random vector x_0 with mean value m_0 and covariance matrix P_0.

The excitation vector $w(t)$ represents a stationary white noise process. The white noise process is Gaussian, it is a Markov process, and its integration yields a Wiener process. The mean vector of the white noise process vanishes,

$$E\left\{w(t)\right\} = 0 \quad , \tag{A-2}$$

and the covariance matrix function is given by

$$E\left\{w(t)w^T(\tau)\right\} = Q\delta(t-\tau) \quad , \quad Q = Q^T \geqslant 0 \quad . \tag{A-3}$$

The spectral density matrix of the stationary white noise process is constant,

$$S_w(\omega) = Q = \text{const} \quad , \tag{A-4}$$

PRECEDING PAGE BLANK NOT FILMED

and the covariance matrix is infinite,

$$E\left\{w(t)w^T(t)\right\} = Q\delta(t,t) \rightarrow \infty \quad . \tag{A-5}$$

This means that the white noise process does not exist in the physical world, but it is an admissible idealization for system analysis similar to the application of impulses in the analysis of deterministic differential equations.

The state vector x(t) characterizes a stochastic process, too, because of the white noise excitation of the system. The solution process is a nonstationary, Gaussian vector process and a Markov process. This means that the solution process can be described by the mean vector,

$$E\left\{x(t)\right\} = \Phi(t,t_0)m_0 \quad , \tag{A-6}$$

and the covariance matrix function,

$$E\left\{x(t)\,x^T(t)\right\} = \Phi(t,t_0)\,P_0\,\Phi^T(t,t_0) + \int_{t_0}^{t} \Phi(t,\tau)\,BQB^T\,\Phi^T(t,\tau)\,d\tau \quad , \tag{A-7}$$

where $\Phi(t,t_0) = e^{A(t-t_0)}$ is the fundamental matrix of A. The mean vector $E\{x(t)\} = m(t)$ and the covariance matrix $E\left\{x(t)\,x^T(t)\right\} = P(t)$ satisfy the differential equations,

$$\dot{m} = Am \quad , \quad m(t_0) = m_0 \quad , \tag{A-8}$$

$$\dot{P} = AP + PA^T + BQB^T \quad , \text{ and } P(t_0) = P_0 \quad . \tag{A-9}$$

Since the system (A-1) is assumed asymptotically stable, the steady-state solutions of the differential equations (A-8) and (A-9) are

$$m_\infty \to 0 \quad , \quad P_\infty = \int_0^\infty e^{As}\, BQB^T\, e^{A^T s}\, ds \quad . \tag{A-10}$$

Thus, the steady-state response of the system (A-1) is characterized by the steady-state covariance matrix P_∞, which can be found by the spectral density analysis or the covariance analysis.

Used in the spectral density analysis is the fact that the steady-state covariance matrix P_∞ can be found as an infinite integral over the spectral density matrix $S_x(\omega)$ of the solution process,

$$P_\infty = \frac{1}{2\pi} \int_{-\infty}^{\infty} S_x(\omega)\, d\omega \quad . \tag{A-11}$$

The spectral density matrix $S_x(\omega)$ can be determined simply by matrix multiplications

$$S_x(\omega) = F(-\omega)\; Q\; F^T(\omega) \quad , \tag{A-12}$$

where

$$F(\omega) = (i\omega E - A)^{-1}\; B \quad . \tag{A-13}$$

Thus, the spectral density analysis is convenient up to the solution of the integral (A-11). However, integral tables are available for the evaluation of the diagonal elements P_{jj} of the covariance matrix, sometimes called variances or squared standard deviations. The variances P_{jj} can always be presented in the following form:

$$P_{jj} = \frac{1}{2\pi i} \int_{-\infty}^{\infty} \frac{g_n(\omega)}{h_n(\omega)\, h_n(-\omega)}\, d\omega \quad , \quad j = 1(1)7 \quad , \tag{A-14}$$

where $g_n(\omega)$ and $h_n(\omega)$ are the polynomials

$$g_n(\omega) = b_0 \omega^{2n-2} + b_1 \omega^{2n-4} + \ldots + b_{n-1} \tag{A-15}$$

and

$$h_n(\omega) = a_0 \omega^n + a_1 \omega^{n-1} + \ldots + a_n = \det(i\omega E - A) \quad . \tag{A-16}$$

A table for the integrals of the form (A-14) is given by James, Nichols, and Phillips [14] for systems of order $n \leqslant 7$.

The covariance analysis uses the linear algebraic covariance matrix equation,

$$AP_\infty + AP_\infty^T + BQB^T = 0 \quad , \tag{A-17}$$

following from the differential equation (A-9) in the steady state. The following theorem on the uniqueness of the solution of equation (A-17) is given by Lancaster [16].

The matrix equation (A-17) has a unique solution if and only if the n^2 numbers

$$\lambda_i + \lambda_j \neq 0 \quad , \quad i = 1(1)n \quad , \quad j = 1(1)n \quad , \tag{A-18}$$

where λ_1 , λ_2 , ... λ_n are the eigenvalues of the matrix A. Since it has been assumed that $\mathrm{Re}\,\lambda_i < 0$ for all $i = 1(1)n$, it follows necessarily that $\lambda_i + \lambda_j < 0$, and, therefore, equation (A-17) has a unique solution.

Although the matrix equation (A-17) is linear in P_∞, its solution cannot be found directly by matrix inversion. However, the expansion in linear equations is possible, according to Chen and Shieh [12]:

$$2Cp + q = 0 \quad . \tag{A-19}$$

The vector p contains the $n(n + 1)/2$ essential elements of the symmetric matrix P_∞, the vector q includes the $n(n + 1)/2$ essential elements of the symmetric matrix BQB^T, and C is the $n(n + 1)/2 \times n(n + 1)/2$ Chen-Shieh matrix. Furthermore, an explicit solution of equation (A-17) has been found by Müller [13]:

$$P_\infty = \frac{1}{2a_0 \det H} \sum_{k=0}^{n-1} H_{k+1,1} \sum_{m=0}^{2k} (-1)^m A_m BQB^T A_{2k-m}^T , \qquad \text{(A-20)}$$

where $A_m = AA_{m-1} + a_m E$ is an $n \times n$-matrix, $a_m = -tr(AA_{m-1})/m$ is the mth coefficient of the characteristic equation, H is the $n \times n$-Hurwitz matrix, and $H_{k+1,1}$ is the cofactor of the element $h_{k+1,1}$ of the Hurwitz matrix.

Both methods, the spectral density analysis and the covariance analysis, can be used to compute the steady-state noise response. However, for systems of higher order, $n > 5$, the covariance analysis makes the computer programing easier because straightforward matrix techniques are available. Therefore, the LST fine pointing system of order $n = 7$ has been investigated by the covariance analysis.

REFERENCES

1. Large Space Telescope Phase A Final Report. NASA TM X-64726, Program Development Directorate, George C. Marshall Space Flight Center, Huntsville, Ala., Dec. 15, 1972.

2. Johns, R.: Pointing Study, Support Module Study, Large Space Telescope. Study Task 46579, Martin Marietta Corp., Denver, Colo., December 1971.

3. Hartter, L.L.; Rybak, S.C.; Mayo, R.A.; and Yeichner, J.A.: A Hard-Mounted Ultrahigh-Accuracy Pointing Control System. AIAA Paper No. 72-854, AIAA Guidance and Control Conference, American Institute of Aeronautics and Astronautics, New York City, 1972.

4. Proise, M.: Fine Guidance Pointing Stability of 120-Inch (3 meter) Large Space Telescope (LST). AIAA Paper No. 72-853, AIAA Guidance and Control Conference, American Institute of Aeronautics and Astronautics, New York City, 1972.

5. Schiehlen, W.: Zustandsgleichungen Elastischer Satelliten. Zeitschrift fuer angewandte Mathematik and Physik, Vol. 23, No. 4, 1972, pp. 575-586.

6. McElvain, R.J.: Satellite Angular Momentum Removal Utilizing the Earth's Magnetic Field. Torques and Attitude Sensing in Earth Satellites, S.F. Singer, ed., Academic Press, New York, 1964, pp. 137-158.

7. Johnson, C.D.: Accommodation of External Disturbances in Linear Regulator and Servomechanism Problems. IEEE Transactions on Automatic Control, Vol. AC-16, No. 6, 1971, pp. 635-644.

8. Johnson, C.D.: Accommodation of Disturbances in Optimal Control Problems. International Journal of Control, Vol. 15, No. 2, 1972, pp. 209-231.

9. Johnson, C.D.: Comments on The Output Control of Linear Time-Invariant Multivariable Systems with Unmeasurable Arbitrary Disturbances. IEEE Transactions on Automatic Control, Vol. AC-17, No. 6, 1972, pp. 836-839.

10. Davison, E.J., The Output Control of Linear Time-Invariant Multivariable Systems with Unmeasurable Arbitrary Disturbances. IEEE Transactions on Automatic Control, Vol. AC-17, No. 5, 1972, pp. 621-629.

11. Porter, B.: Stability Criteria for Linear Dynamical Systems. Academic Press, New York, 1968.

REFERENCES (Concluded)

12. Chen, C.F.; and Shieh, L.S.: A Note on Expanding $PA + A^TP = -Q$. IEEE Transactions on Automatic Control, Vol. AC-13, No. 1, 1968, pp. 122-123.

13. Müller, P.C.: Solution of the Matrix Equation $AX + AB = -Q$ and $S^TX + XS = -Q$. SIAM Journal of Applied Mathematics, Vol. 18, No. 3, 1970, pp. 682-687.

14. James, H.M.; Nichols, N.B.; and Phillips, R.S.: Theory of Servomechanisms. McGraw-Hill Book Co., New York, 1947.

15. Bucy, R.S.; and Joseph, P.D.: Filtering for Stochastic Processes With Application to Guidance. Interscience Publishers, John Wiley & Sons, Inc., New York, 1968.

16. Lancaster, P.: Theory of Matrices, Academic Press, New York, 1969.

APPROVAL

A FINE POINTING SYSTEM FOR THE LARGE SPACE TELESCOPE

By Werner O. Schiehlen

The information in this report has been reviewed for security classification. Review of any information concerning Department of Defense or Atomic Energy Commission programs has been made by the MSFC Security Classification Officer. This report, in its entirety, has been determined to be unclassified.

This document has also been reviewed and approved for technical accuracy.

Hans H. Hosenthien

HANS H. HOSENTHIEN
Chief, Research and Development Analysis Office

F. B. Moore

F. B. MOORE
Director, Astrionics Laboratory

NASA-Langley, 1973 — 30 M217